

Student number : 0581204

**Isolation of a novel inhibitor of osteoclastogenesis and its
functional analysis *in vitro* and *in vivo***

Anton Bahtiar

Nara Institute of Science and Technology

Graduates School of Biological Sciences

Laboratory of Molecular Oncology

(Prof. Tatsuo Takeya)

Submitted January 22, 2010

Abstract

Osteoclasts are multinucleated giant cells with bone-resorbing activity and play a key role in bone remodeling in conjunction with osteoblasts. They originate from hematopoietic stem cells, which differentiate into osteoclasts through a series of steps involving the commitment of hematopoietic stem cells to the monocyte/macrophage lineage, proliferation of preosteoclasts, and differentiation into mature osteoclasts with resorptive activity. It is well established that receptor activator of NF- κ B ligand (RANKL) plays a central role in osteoclastogenesis through its cognate receptor activator of NF- κ B (RANK).

Our group previously found, using an *in vitro* model of osteoclastogenesis consisting of mouse cells and recombinant RANKL, that the expression of the transcription factor NFAT2 (NFATc1) induced by stimulation with RANKL is essential for the formation of mature osteoclasts. Interestingly, culture at high cell density blocked progression to the multinucleated cell stage. Subsequently, high cell density was found to cause a change in the composition/state of the culture medium accompanying a downregulation of NFAT2 expression, and we eventually identified L-Ser as a key component for the phenomenon. Although the differentiation medium contained seven nonessential amino acids (L-Ala, L-Asn, L-Asp, L-Glu, L-Gly, L-Pro and L-Ser), only L-ser had such a characteristic effect. In fact, no osteoclasts formed when L-Ser alone was removed from the differentiation medium with

dialyzed serum, and in contrast, the presence of only L-Ser was sufficient to induce NFAT2 expression and the formation of osteoclast. These findings implied a specific role of L-Ser in osteoclasts and at the same time, suggested the possibility of using certain analogs to suppressing osteoclastogenesis through the downregulation of NFAT2 expression.

In this study, I systematically searched for L-Ser analogs with suppressive activity and less toxicity. I screened about a hundred substances and consequently identified a novel serine analog, H-Ser(tBu)-OMe • HCl (or O-t.-Butyl-L-Serine methyl ester hydrochloride), which suppressed osteoclastogenesis *in vitro* by downregulating RANK expression as well as its localization in membrane lipid rafts and the subsequent RANKL/RANK signaling cascade. The analog appeared to inhibit the production of 3-ketodihydrosphingosine by serine palmitoyltransferase (SPT), and the addition of lactosylceramide rescued the osteoclast forming process. An analysis using the analog thus shed light on the significance of serine metabolism through SPT in osteoclastogenesis. Moreover, this effect was confirmed *in vivo*; namely, administration of the analog appeared to increased bone density in control mice and to prevent high bone turnover in soluble RANKL-treated mice. Therefore, the findings may be useful for developing a novel therapeutic tool for bone diseases such as osteoporosis, which is known to be accelerated by enhanced bone-resorbing activity and/or the formation of osteoclasts.

Contents

Abstract	2
Contents	4
I. Introduction	6
I.1. Bone	6
I.2. Bone Remodeling	13
I.3. Molecular mechanism of osteoclastogenesis.....	15
I.4. L-Serine	18
I.5. D-Serine.....	20
I.6. Sphingolipids	21
I.7. Osteoporosis.....	23
I.8. Purpose of this research.....	26
II. Materials and Methods	27
II.1. Cells and reagents.....	27
II.2. Cytotoxicity assay.....	27
II.3. Isolation of bone marrow cells and osteoclastogenesis.....	28
II.4. Immunoprecipitation and western blotting.....	29
II.5. Screening of amino acids and their derivatives.....	29
II.6. Acute toxicity studies.....	29
II.7. Induction of high bone turnover.....	30
II.8. Peripheral quantitative computer tomography analysis (pQCT).....	30
II.9. Histomorphometric analysis.....	31
II.10. Preparation of Serine Palmitoyltransferase (SPT) and SPT assay.....	31
III. Results	32
III.1. Screening of amino acids and their derivatives.....	33
III.1.a. #290 inhibited osteoclastogenesis in a dose-dependent manner	34

III.1.b. #290 downregulated the RANKL/RANK signaling cascade.....	35
III.2. Analysis of the function of #290 in L-Ser metabolism.....	37
III.2.a. L-Ser metabolism is important for osteoclastogenesis.....	37
III.2.b. #290 inhibits SPT activity.....	37
III.3. <i>in vivo</i> experiments using normal and osteoporotic mice.....	40
III.3.a. LD50 test of #290.....	40
III.3.b. Effects of #290 on normal mice	41
III.3.c. Preparation of osteoporotic-model mice.....	41
III.3.d. Effects of #290 on osteoporotic-model mice.....	42
IV. Discussion.....	43
V. Figures and legends	47
VI. Acknowledgements.....	74
VII. References.....	75

I. Introduction

I.1. Bone

I.1.a. Anatomy and structure of bone

Bone is a complex dynamic tissue that together with cartilage forms the skeletal system. The skeleton provides mechanical support for the body and site of muscle attachment for locomotion as well as protection for vital organs. Bone is highly vascularized, contains hematopoietic bone marrow and provides a reserve of ions, especially calcium and phosphate. Anatomically, bones can be divided into two major types: flat bones (calvaria and facial bones, scapula, mandible, sternum, etc) and long bones (tibia, femur, humerus, etc.). Morphologically, bones can be divided into two forms: cortical (compact) and trabecular or cancellous (spongy). These forms have both structural and functional differences. Cortical bone mainly has mechanical and protective functions, whereas trabecular bone also has metabolic functions e.g. in calcium homeostasis (Kierszenbaum, 2007).

A long bone consists of a shaft or diaphysis, and two epiphyses at the ends of the diaphysis. A metaphysis links each epiphysis to the diaphysis. During bone growth, a cartilaginous growth plate is present at the epiphysis-metaphysis interface but after growth, a residual growth line replaces the growth plate. The diaphysis is surrounded by a cylinder of compact bone containing the bone marrow. The epiphyses consist of spongy or

cancellous bone covered by a thin layer of compact bone. The periosteum covers the outer surface of the bone, whereas the endosteum lines the marrow cavity.

I.1.b. Bone formation and growth

Two distinct types of developmental processes, intramembranous and endochondral form flat and long bones, respectively.

Intramembranous ossification

Intramembranous ossification occurs during embryonic development and starts with the migration and condensation of mesenchymal cells. The cells of these condensations differentiate directly into bone-forming osteoblasts. The first bone is formed as an immature irregular matrix, which calcifies into woven bone. The mesenchymal cells continue to differentiate in the periphery, the matrix becomes vascularized, and bone marrow is formed. The woven bone is subsequently remodeled and replaced by mature lamellar bone (Figure 1).

Endochondral ossification

Endochondral ossification is the process by which templates of skeletal cartilage are replaced by bone. The process begins with the proliferation and aggregation of mesenchymal cells at the site of future bone. These mesenchymal cells differentiate into chondroblasts that secrete cartilage matrix leading to the development of a cartilage model. The chondroblasts become embedded within their own matrix, and thereafter are called

chondrocytes. Perichondrial cells become osteoblasts, which form a thin bone collar surrounding the future diaphysis. As a result of these changes, the perichondrium is transformed into the periosteum. In the mid-diaphyseal region, chondrocytes become hypertrophic, and synthesize alkaline phosphatase, which is followed by calcification of the matrix. The hypertrophic chondrocytes undergo apoptosis, and the matrix breaks down, producing a growing cavity (Figure 2). Meanwhile, blood vessels grow into the cavity and come in contact with bone marrow cells. The calcified matrix is partially resorbed and osteoblasts begin to lay down osteoid. This area is called the primary ossification center. In late fetal life and early childhood, secondary ossification centers form in the upper epiphyses in a similar manner (Kronenberg, 2003)

The growth plate

The growth plate (or epiphyseal plate), located below the secondary ossification center, is the site of longitudinal growth of long bones. Four major zones can be distinguished. The reserve zone (or resting zone) is a source of mesenchymal stem cells. The proliferative zone is characterized by active proliferation of chondrocytes, arrangement of the cells in vertical stacks and formation of matrix. In the hypertrophic zone, the chondrocytes become progressively larger, separate from each other and then undergo apoptosis. In the calcifying zone, the remaining longitudinal septae of cartilages are subsequently calcified. The calcified matrix is partially resorbed by chondroclast. Blood vessels penetrate the transverse

septae and carry osteoprogenitor cells. These cells differentiate and form a layer of woven bone on top of the cartilaginous remnants of longitudinal septae, and the primary spongiosa is generated. This woven bone is later further remodeled, in which the woven bone and the cartilage remnants are replaced with lamellar bone, resulting in mature trabecular bone called secondary spongiosa. Growth plate inactivation occurs at puberty as a result of an increase in secretion of estrogen in both males and females, and the growth plates are replaced by trabecular bone leading to cessation of growth.

Bone matrix

The bone is composed of an organic matrix, that is strengthened by deposits of inorganic hydroxyapatite [$\text{Ca}_{10}(\text{PO}_4)_6(\text{OH})_2$], and a cellular phase. The organic bone matrix contains type I collagen fibers, non-collagenous proteins, serum proteins and proteoglycans. The most predominant protein of the bone matrix is type I collagen (90%). Type I collagen fibers consist of triple-helical molecules packed into microfibrils with the help of intermolecular crosslinks. The fibrils are further packed into collagen fibers forming a highly ordered structure providing elasticity and flexibility to bone (Knott, 1998). Collagen determines the toughness of bone, while the mineral confers stiffness. The balance of these two properties of bone determines its overall strength. Cortical bone is calcified 80-90%, whereas trabecular bone is calcified 15-25% (Karsenty, 2003).

The extracellular matrix (ECM) of bone contains a relatively small amount of

non-collagenous protein; however, it controls a variety of bone-specific functions including the regulation of mineralization, cell adhesion and bone resorption/remodeling.

Bone mineralization

Bone collagen can be regarded as a scaffold on which mineral deposition occurs. Many non-collagenous matrix proteins (NCP) are acidic in nature and bind to the bone matrix because of their affinity for hydroxyapatite. These non-collagenous matrix proteins actively control the mineralization of collagen fibers and crystal growth within the osteoid when it is converted to bone. The crystals are transported in membrane-bound extracellular vesicles, known as ECM or matrix vesicles, released from chondrocytes and osteoblasts, and distributed along the length of collagen fibers and into the ground substance. The ground substance, composed of glycoproteins and proteoglycans, consists of highly anionic complexes with a high ion binding capacity and thus participates in the calcification process and in the fixation of hydroxyapatite crystals to the collagen (Knott, 2003). The ECM vesicles accumulate calcium and phosphate ions, and contain enzymes that can degrade inhibitors of mineralization, e. g. adenosine triphosphate (ATP), pyrophosphate (PPi) and proteoglycans, present in the surrounding matrix. They also contain a nucleation core, consisting of protein and a complex of acidic phospholipids, calcium, and inorganic phosphate, which can induce apatite to form (Boskey, 1997). Alkaline phosphatase (ALP) is an enzyme important for mineralization. ALP hydrolyzes phosphate esters, increasing the

local phosphate concentration, and enhancing the rate and extent of mineralization. ALP also hydrolyzes inhibitors of mineral deposition such as pyrophosphate.

I.1.c. The cellular components of bone

Osteoblasts

Osteoblasts are bone-forming cells, responsible for synthesis of the organic matrix, the osteoid, and subsequently control mineralization of the matrix (Marks, 1988). An equally important function of osteoblasts and preosteoblasts is the regulation of osteoclastic differentiation and resorption via the OPG/RANK/RANKL-system. Osteoblasts originate from mesenchyme-derived osteoprogenitor cells present in the inner layer of the periosteum and the endosteum. Osteoprogenitor cells persist throughout postnatal life as bone-lining cells with the capacity to be reactivated in adulthood during the repair of bone fractures and other injuries.

After deposition of the bone matrix, the terminal stages of osteoblast differentiation result in three fates for these cells: they may become inert bone-lining cells, become trapped in the mineralized matrix forming osteocytes, or undergo apoptosis. Osteoblasts are epithelial-like cells with cuboidal shapes, forming a monolayer covering all sites of active bone formation. Osteoblasts display features typical of cells active in protein synthesis. Morphologically, they are characterized by a round nucleus, a large rough endoplasmic

reticulum, an extensive Golgi apparatus and some lysosomal-like bodies (Marks, 1988). Bone-lining cells are flattened and elongated, are characterized by a moderately large rough endoplasmic reticulum and Golgi apparatus, and stain immunohistochemically positive for intercellular adhesion molecule-1 (ICAM-1). Differentiated osteoblasts are highly enriched in alkaline phosphatase that disappears when the cells become embedded in the matrix as osteocytes. They also synthesize protein such as type I collagen, osteocalcin, OPN and BSP (Knott, 1998).

The osteocytes

Osteoblasts differentiate into osteocytes after becoming trapped in lacunae within the mineralized matrix they produce. It has been suggested that 10-20% of osteoblasts differentiate into osteocytes. These cells form an extensive network of small channels, the canaliculi, which interdigitate through the lamellae and connect neighboring lacunae. The network of osteocytes provides intracellular communication across gap junctions, thus osteocytes are in direct communication with osteoblasts, osteoclasts and surface-lining cells. Moreover, canaliculi connecting osteocyte lacunae also provide the cells with nutrients and signaling molecules from the extra cellular environment. It has been suggested that osteocytes play a role as mechanosensors and in local activation of bone turnover. The osteocyte expresses receptors for most of the hormones and cytokines known to be important in bone function, including estrogen receptors, PTH, 1,25-vitamin D3, corticosteroids and

transforming growth factor- β (TGF- β). A molecule typically expressed in osteocytes is DMP-1. DMP-1 acts as a nucleator of hydroxyapatite formation and is critical for the proper mineralization of bone (Kalajnic, 2004).

Osteoclasts

Osteoclasts are multinucleated cells responsible for bone resorption and the mobilization of calcium. The osteoclast precursor is a member of the monocyte-macrophage lineage present in the adjacent bone marrow (Baron, 1989). Osteoclasts are ultrastructurally characterized by multinuclearity, an abundance of mitochondria and cytoplasmic vesicles, and the expression of specialized membrane domains on the apical surface facing the bone.

I.2. Bone remodeling

Remodeling is the process by which bone is turned over, allowing maintenance of the shape, quality and size of the skeleton. Bone remodeling serves to modify the structure of bone in response to changes in mechanical needs and to repair microdamage in the bone matrix, preventing the accumulation of old bone. During adulthood, about 10% of bone is replaced each year with complete renewal every 10 years. Bone deposition and bone resorption are ongoing dynamic processes. Osteoclasts and osteoblasts closely collaborate in the remodeling process in what is called a basic multicellular unit (BMU). The organization of BMUs differs between cortical bone and trabecular bone, but these differences are mainly

morphological rather than biological. Between 2 and 5% of cortical bone is remodeled each year, whereas trabecular bone is more actively remodeled due to a much larger surface to volume ratio. The complete remodeling cycle at a specific site takes about 3-6 months. Bone resorption is a faster process than bone formation. Bone resorption occurs in weeks, but bone formation takes months, explaining why sites of resorption are less common than sites of formation (Figure 4).

Remodeling can be divided into four phases; 1) osteoclastic bone resorption, 2) release of osteoclasts and cleaning of the resorption cavity, 3) osteoblastic action with the formation of the osteoid, and 4) mineralization of the osteoid. There normally a balance between resorption and formation, and any imbalance can have serious consequences. In bone remodeling, the term coupling is defined as the strictly regulated replacement of old bone with the same amount of new bone. Molecular communication between osteoblasts and osteoclasts and between bone cells and other bone marrow cells couples precisely bone formation with resorption. The OPG/RANK/RANKL system allows crosstalk between osteoblastic and osteoclastic cells. Most skeletal disorders are caused by uncoupling in this remodeling process, favoring either bone resorption or bone formation, such as osteoporosis or osteopetrosis (Mundy, 2001)

I.3. Molecular mechanism of osteoclastogenesis

The transcription factors, PU.1 and MITF, acting early in the monocyte-macrophage lineage, regulate the development of hematopoietic precursor cells and committed precursors into osteoclasts (Celadon, 1996). Mice deficient in PU.1 lack osteoclasts as well as macrophages and thus develop osteopetrosis (Tondratovi, 1997). Initial experiments by Soda, revealed that the generation of osteoclasts in culture require physical contact between the precursor cells and specific mesenchymal cells such as osteoblasts or marrow stromal cells. It is now clear that macrophage colony stimulating factor (M-CSF) and receptor activator of nuclear factor- κ B ligand (RANKL), both expressed in osteoblasts or stromal cells, are essential for osteoclastogenesis. In fact, the generation of pure populations of osteoclasts in vitro is achieved by culturing marrow macrophages in the presence of only RANKL and M-CSF (Teitelbaum, 2007).

Secreted M-CSF binds to the receptor c-fms, a tyrosine kinase that activates ERK 1/2 and PI3K/AKT. This signaling pathway promotes the proliferation of osteoclast precursor cells and survival of the differentiated osteoclast. The critical importance of M-CSF in osteoclast recruitment has been illustrated in the *op/op* mouse, which lacks a functional M-CSF and has osteoclast-deficient osteopetrosis (Teitelbaum, 2007).

Using a series of genetically modified mice, it has been clearly demonstrated that RANKL and its receptor RANK are indispensable for osteoclastogenesis (Theil et al. 2002).

The factor that directly controls the differentiation process is now assumed RANKL: molecular events during osteoclastogenesis have thus come to be understood in the context of RANKL–RANK signaling.

RANK lacks intrinsic enzymatic activity in its intracellular domain, and the analyses of molecules associated with the cytoplasmic domain of RANK revealed that it transduces signals by recruiting adaptor molecules such as the TRAF family of proteins (Darnay et al., 1998, Galibert et al., 1998). The TRAF family contains seven members (TRAFs 1, 2, 3, 4, 5, 6 and 7) and mainly mediates signaling induced by TNF family cytokines and pathogen-associated molecular patterns (PAMPs) (Inoue et al., 2000). The cytoplasmic tail of RANK contains three TRAF6-binding sites and two sites for the binding of other TRAF family members including TRAF2, TRAF3 and TRAF5 (Darnay et al., 1999, Galibert et al., 1998, Gohda et al., 2005).

The binding of TRAF6 to RANK induces the trimerization of TRAF6, leading to the activation of NF- κ B and mitogen-activated kinases (MAPKs) (Kobayashi et al., 2001, Lomaga et al., 1999, Wong et al., 1998). TRAF6 contains an N-terminal RING finger domain and a stretch of predicted zinc finger domains. The ubiquitin ligase activity mediated by the RING finger motif of TRAF6 has been shown to be important for NF- κ B's activation in other cell types (Deng et al.2000).

RANK activates the transcription factor complex AP-1 partly through an induction of

its critical component, c-Fos (Takayanagi et al., 2002, Wagner et al., 2005). AP-1 is a dimeric complex composed of the Fos (c-Fos, FosB, Fra-1, Fra-2), Jun (c-Jun, JunB, JunD) and ATF (ATFa, ATF2, ATF3, ATF4, B-ATF) proteins. Mice lacking c-Fos develop severe osteopetrosis due to a complete block of osteoclastic differentiation. It was reported that transgenic mice expressing dominant negative c-Jun under the control of the *TRAP* promoter exhibited osteopetrosis (Ikeda et al., 2004). Since the dominant negative c-Jun inhibits AP-1 activity by binding to the Fos, Jun and ATF families of proteins, this transgenic mouse confirms that AP-1 activity is critical for osteoclastogenesis.

In a genome-wide search for the RANKL-inducible genes specifically required for the terminal differentiation of osteoclasts, NFATc1 was shown to be strongly induced by RANKL (Ishida et al., 2002, Takayanagi et al., 2002). NFATc1 expression is dependent on the TRAF6-NF- κ B and c-Fos pathways, which are activated by RANKL, suggesting an integral role for NFATc1 in RANKL signaling. The NFAT transcription factor family was originally identified in T cells and is now comprised of five members including NFATc1 (NFAT2), NFATc2 (NFAT1), NFATc3 (NFAT4), NFATc4 (NFAT3) and NFAT5. This family developed along with the evolution of the vertebrates, and is involved in the regulation of a variety of biological systems such as the cardiovascular and muscular systems in addition to the immune system. The activation of NFATc1/c2/c3/c4 is mediated by a specific phosphatase, calcineurin, which is activated by calcium/calmodulin signaling. Consistent with this,

calcineurin inhibitors such as FK506 and cyclosporin A strongly inhibit osteoclastogenesis. The necessary and sufficient role of *NFATc1* in osteoclastogenesis was suggested by the *in vitro* observation that *NFATc1*^{-/-} embryonic stem cells do not differentiate into osteoclasts and the finding that ectopic expression of NFATc1 causes bone marrow-derived precursor cells to undergo osteoclast differentiation in the absence of RANKL .

I.4. L-SERINE

L-Ser, one of the so-called non-essential amino acids, plays a central role in cellular proliferation. Besides its role in protein synthesis, L-Ser serves as a metabolic precursor/intermediate necessary for various pathways of biosynthesis. These include the production of glycine, L-cysteine, phosphatidylserine (PS), sphingolipids, and D-serine an activator of the N-methyl-D-aspartate (NMDA)-selective glutamate receptor (Figure 7). Furthermore, L-Ser participates indirectly in the biosynthesis of purines and pyrimidines by transferring a methylene group (C3-serine) to tetrahydrofolate (THF) (Koning et al., 2003). L-Ser's metabolism in animal cells has been well characterized, and its *de novo* synthesis in the brain is thought to be important, because of its low ability to cross at the blood-brain barrier. The biosynthesis of L-Ser from a glycolytic intermediate, 3-phosphoglycerate, involves three sequential reactions initiated by 3-phosphoglycerate dehydrogenase (3PGDH) (Ichihara et al., 1957, Snell et al., 1984). L-Ser is also converted from gly by serine

hydroxymethyltransferase. Indeed, these enzymes are widely distributed in various organs including the brain, and significantly upregulated in their expression in proliferating cells and neoplastic tissues. Serine-deficiency disorders involve rare defects in the biosynthesis of L-Ser. Two such disorders have been reported to date, one involving a lack of 3-phosphoglycerate dehydrogenase and the other, a lack of 3-phosphoserine phosphatase. Defects in these enzymes lead to severe neurological symptoms such as congenital microcephaly and severe psychomotor retardation. In addition, lack of 3-phosphoglycerate dehydrogenase can lead to intractable seizures. These symptoms respond to some degree to treatment with L-Ser, sometimes combined with gly.

Previously we found that a high cell density in the *in vitro* system blocked progression to the multinucleated cell stage even in the presence of RANKL. A high cell density appeared to cause a change in the composition of the culture medium accompanying downregulation of NFAT2 expression, and we subsequently identified L-Ser as a key component for this effect. Namely, the high cell density caused a depletion of L-Ser in the medium and this turned out to be the major reason for the suppression of multinucleated cell formation. Conversely, removal of only L-Ser from the differentiation medium halted osteoclastic formation without affecting cell viability, and the addition of NFAT2 could rescue the osteoclastogenesis. Although the differentiation medium contained seven amino acids (Ala, Asn, Asp, Glu, Gly, Pro, and Ser), only L-ser had this characteristic effect. Thus, we

identified a novel role for L-Ser in osteoclastogenesis (Ogawa et al., 2006).

I.5. D-Serine

For a long time, researchers ignored D-amino acids, because they have a less biologically active conformation than L-amino acids. Although D-amino acids were confirmed to exist in bacteria, worms and other invertebrates, it was several years before they were detected at high levels in mammalian tissues, especially in the brain. Among the first to be discovered in high concentrations in the brain was D-Asp (Dunlop et al., 1986). Later on, another very important D-amino acid called D-serine was found at elevated levels in the mammalian brain (Hashimoto et al., 1993).

D-ser is synthesized from L-Ser in one enzymatic step catalyzed by serine racemase (Schell et al., 2004). This enzyme is proposed to be the main, if not only, endogenous source of D-Ser. The serine racemase also catalyzes the conversion of D-Ser into L-Ser, albeit with less affinity. The serine racemase has a similar distribution is analogs to D-Ser, with highest levels in the forebrain.

D -Ser has been demonstrated to exist naturally in the brain (Hanada et al., 2000), where sphingolipids are relatively abundant. Thus, in the present study, the stereochemical specificity of the substrate for SPT was examined, and D -Ser was found to be a competitive inhibitor of L -Ser in the SPT reaction. Serine palmitoyltransferase (SPT), responsible for

the initial step of sphingolipid biosynthesis, catalyzes the condensation of palmitoyl coenzyme A and L-Ser to produce 3-ketodihydrosphingosine (KDS). The recognition of L-Ser by SPT is likely to involve the formation of a Schiff-base between the amino acid substrate and a pyridoxal phosphate-group in the enzyme. The binding of both enantiomers of a compound to one enzyme is exceptional, but not inconceivable for pyridoxal phosphate-dependent enzymes. For example, serine racemase, a pyridoxal phosphate-dependent enzyme, recognizes both L- and D-serine, and catalyzes the conversion of L-serine to D-serine and vice versa. Thus, the SPT enzyme is presumably able to form Schiff-base complexes with both enantiomers of serine, although in the postulated subsequent reaction, substitution of the α -hydrogen atom of serine with the palmitoyl group of palmitoyl CoA may proceed in the Schiff-base complex with L-serine but not D-serine (Hanada et al., 2000)

I.6. Sphingolipids

Sphingolipids represent a class of membrane lipids that contain a hydrophobic ceramide chain as a common backbone structure. Sphingolipid synthesis requires two simple components: L-Ser and palmitoyl CoA. Although L-Ser is classified as a non-essential amino acid, an external supply is essential for the synthesis of sphingolipids and phosphatidylserine (PS) in particular types of central nervous system (CNS) neurons (Hannun

et al., 2008)

Sphingolipids are synthesized *de novo* from serine and palmitate, which condense to form 3-KDS through the action of SPT (Figure 8). In turn, 3-KDS is reduced to dihydrosphingosine, followed by acylation by a (dihydro)-ceramide synthase (also known as Lass or CerS). Ceramide is formed by the desaturation of dihydroceramide.

In sphingolipid biosynthetic pathways, ceramide can be phosphorylated by ceramide kinase, glycosylated by glucosyl or galactosyl ceramide synthases, or receive a phosphocholine headgroup from phosphatidylcholine (PC) in the biosynthesis of sphingomyelin (SM) through the action of SM synthases, which thereby also serve to generate DAG from PC.

The breakdown of complex sphingolipids proceeds through the actions of specific hydrolases, leading to the formation of glucosylceramide and galactosylceramide. In turn, specific β -glucosidases and galactosidases hydrolyse these lipids to regenerate ceramide. One of several sphingomyelinases (SMases) catalyzes the breakdown of SM. These include acid SMase, neutral SMases and alkaline SMase.

Glycosphingolipids are thought to play important roles in the development and function of several tissues, although the function of glycolipids in osteoclastogenesis has not been clearly demonstrated. In the present study,

D-threo-1-phenyl-2-decanoylamino-3-morpholino-1-propanol (D-PDMP), a glucosylceramide

synthase inhibitor, completely inhibited osteoclastogenesis induced by M-CSF and RANKL. Following treatment with D-PDMP, the expression of nearly all glycosphingolipids was dramatically reduced on the surface of bone marrow cells, which suggests that glycosphingolipids are necessary for osteoclastogenesis (Iwamoto et al., 2001, Fukumoto et al., 2006)

I.7. Osteoporosis

Osteoporosis has been defined as “a disease characterized by low bone mass and microarchitectural deterioration of bone tissue leading to enlarged bone fragility and a consequent increase in fracture risk”. Osteoporosis is most frequently caused by continuous, physiological, gender and age-related, systemic bone loss after the menopause in women and in men above the age of 50 years. The incidence of osteoporosis in a population is dependent on gender, age, endocrine status, lifestyle and menopausal age, the highest risk group being white postmenopausal women (Wower, 2001). Bone loss can be slowed or even reversed if risk factors such as physical inactivity, low dietary calcium intake, and primary hyperparathyroidism are identified and reversed. The rate of bone resorption exceeds the rate of bone formation in older adults, resulting in “too little bone within the bones” and osteoporosis.

The rate of bone loss (in percent) is about twice as high in older women as in men of

the same age. About 25% of the early postmenopausal population may lose between 5 and 8% per year. Hormones and drugs affect different regions of the skeleton in different ways, e.g., estrogen deficiency and glucocorticoid therapy result primarily in cancellous bone loss, whereas parathyroid hormone excess results primarily in cortical bone loss. The regional differences may also be dependent on whether the bone is subjected to weight-bearing stresses or not and whether the bones contain red marrow or yellow marrow.

Nowadays the commonly accepted methods for BMC/BMD measurements are dual-photon (DPA) and dual X-ray energy absorptiometry (DXA), which minimize the influence of inter- and intraindividual variations in soft tissue thickness. In contrast, quantitative computed tomography (QCT) measures volumetric density and the results are given in grams per cubic centimeter. When using suitable software, peripheral QCT (pQCT) permits different factors to be examined separately, i.e., the density of the cancellous bone and the pattern of the cancellous microtexture, as well as the cortical bone density and width (Frost HM, 1998). In daily clinical practice the most useful method for BMD assessments in the vertebrae, femoral neck, and forearms is DXA, as it is faster, more precise, accurate and cheaper than any other method.

It is advisable to treat postmenopausal females who are exposed to the highest risk of osteoporosis and, thus, for fractures (Eastell R, 1998). Estrogen replacement therapy is the first choice of treatment. This results from long-term experience based on randomized,

controlled trials, cohort studies and cross-sectional studies. This therapy is also chosen because of its other benefits (relief of menopausal symptoms, prevention of ischemic heart disease and dementia) besides the prophylactic treatment against fast BMC loss (Gorai et al., 1999). The treatment should be administered for at least 5 years and preferably much longer because the benefits may not persist after treatment is stopped (George et al, 1999). Moreover, lifestyle changes, including exercise and the use of hip protectors in frail older females calcium (1 g/day), combined with vitamin D3 (14 g/day) should be given to all postmenopausal women. This supplement partially reverses the age-related increase in serum parathyroid hormone levels and bone resorption and decreases bone loss (Baeksgaard et al., 1998). A class of bisphosphonates are selective inhibitors of bone resorption. These drugs are now recommended as an effective alternative to estrogen replacement therapy in women who are concerned about the adverse effects of estrogen therapy (Eastell, 1995). These bisphosphonates are absorbed in newly formed bone and buried in bone for years. They reduce the activity of individual osteoclasts, reduce the activation frequency by inhibiting recruitment and differentiation of osteoclast precursors, and accelerate osteoclast apoptosis (Geddes et al., 1994). However, it is important to note that bisphosphonates are still under evaluation in clinical trials and new information could alter the recommendations about their status.

I.8. Purpose of this research

We examined the specificity with which L-Ser induces NFAT2 expression using D-Ser and L-homoserine. Neither analog, however, could substitute for L-Ser. Instead, when each was added together with L-Ser, there was a suppressive effect on NFAT2 expression, implying such analogs to be useful for suppressing osteoclastogenesis through the downregulation of NFAT2 expression. However, the analogs showed some toxicity. On such background, the purpose of my study is to search novel compound(s) that function as an osteoclastogenic inhibitor, to investigate the functional mechanism of compound(s) and to analyze the effects on bone turnover *in vivo*

II. Materials and Methods

II.1. Cells and reagents

RAW264 cells were cultured in Eagle's minimum essential medium (EMEM; Nissui, Tokyo, Japan) supplemented with non-essential amino acids (GIBCO-BRL, NY, USA), 0.1 mM L-Gln (Nissui) and 10 % fetal bovine serum (FBS). GST-RANKL was prepared as described previously (Ishida et al., 2002). The anti- β -actin monoclonal antibody (AC-74) was purchased from Sigma-Aldrich Japan (Tokyo, Japan). Rabbit anti-ERK and anti-pERK, and anti-p38 and anti-phospho p38 antibodies were from Promega (WI, USA) and Cell Signaling Technology. The anti-RANK antibody (sc-9072), anti-NFAT2 monoclonal antibody (sc-7294) and anti-c-Fos (sc-52) rabbit polyclonal antibody were obtained from Santa Cruz Biotechnology (CA, USA). HRP-conjugated sheep anti-mouse IgG and HRP-conjugated protein-A were purchased from GE Healthcare UK Ltd. FB1 and Myriocin were obtained from Calbiochem (CA, USA). Lactosylceramide and H-Ser(tBu)-OMe-HCl were purchased from Sigma-Aldrich and Merck, respectively.

II.2. Cytotoxicity Assay

The cytotoxicity of L-ser analogues was assayed with Cell Counting Kit-8 (Dojindo Laboratories, Kumamoto, Japan). Cells were incubated in 96-well plates at a density of 2×10^4 cells/well in triplicate in the presence of increasingly higher concentrations of L-Ser

analogues. After 72 hrs, 10 μ l of the solution of Cell Counting Kit-8 was added to each well and the cells were incubated for another two hrs. The absorbance of each well was measured at 450 nm.

II.3. Isolation of bone marrow cells and osteoclastogenesis

For osteoclastogenesis *in vitro*, either RAW264 cells or bone marrow macrophages (BMM) were seeded at 5×10^4 cells/ml and incubated for 24 hrs. Purified GST-RANKL or GST, prepared as described previously (Ishida et al., 2002), was added to the culture medium at final concentration of 400-500 ng/ml (RANKL) or 200 ng/ml (GST). The medium was changed every 3 days with Eagle medium containing RANKL or GST. BMM were prepared as described previously (Ogawa et al., 2006) with some modifications. In brief, bone marrow cells were collected by flushing the femurs and tibias of 6 to 8-week old wild-type mice with minimum essential medium alpha (α -MEM; GIBCO-BRL), and red blood cells were removed by treatment with an ammonium chloride solution. After a wash, the cells were cultured in α -MEM supplemented with 10% fetal bovine serum (FBS). After 12-16 hours, non-adherent cells were collected and cultured a further 1-3 days in α -MEM supplemented with 10% FCS and 100 ng/ml of M-CSF.

II.4. Immunoprecipitation and Western blotting

Cells were lysed with RIPA buffer (10 mM Tris-HCL, 1% NP40, 0.1% Deoxycholic acid, 0.1% SDS, 150 mM NaCl, and 1 mM EDTA) containing 2 mM PMSF, 2 mM Na₃VO₄, 20 mM NaF, and 100 KIU/ml of aprotinin. Immunoprecipitation and Western blotting were carried out essentially as described previously (Ogawa et al., 2006) using protein A-Sepharose (GE Healthcare Bioscience KK, Tokyo, Japan). The proteins were separated by SDS-PAGE, transferred to a PVDF membrane (Millipore, MA, USA), and detected by Western blotting using an ECL detection kit (GE Healthcare Bioscience KK, Tokyo, Japan)

II.5. Screening of amino acids and their derivatives

We collected 100 L-Ser analogs including dipeptides. Substances that caused cell death or showed osteoclast-inducing activity were eliminated at the first screening. Candidates were then added at concentrations of 0.1 mM, 1 mM, and 10 mM to the culture of *in vitro* system described above, and numbers of TRAP-positive multinucleated cells formed were counted after 4 days.

II.6. Acute toxicity study in mice

Test substances were administered intraperitoneally to a group of female mice (n=5). Dose levels were selected in such a way that 0-100% of the animals will die. LD₅₀ values

with 95% confidence limits and function were determined based on the table of Fisher and Yates (Akhila et al., 2007).

II.7. Induction of high bone turnover in mice

This experiment was carried out essentially as described (Williams et al., 1984). C57BL/6Jc1 female mice, aged 7 weeks, were intraperitoneally injected with 100 μ g of GST or GSST-RANKL three times at intervals of 24 hrs. L-Ser analogs were injected twice a day with the first injection 1 hr before GST-RANKL treatment and the second injection 8 hrs after the first. One day after the last injection, all of mice were sacrificed and subjected to pQCT and microCT examinations.

II.8. Peripheral quantitative computer tomography (pQCT)

The right tibia was dissected out to be examined as described above, and stored in 70 % ethanol. The distal metaphysis and midshaft of each tibia sample were scanned with a pQCT system (XCT Research SA+, Norland Stratec Medizintechnik GmbH). The growth cartilage at the distal epiphysis of the tibia was used as a reference line, and 2 sites, 1 mm and 7 mm medial to the line, were selected as the point of analysis for trabecular and cortical BMD, respectively. The following setup was used for the measurement; voxel size = 0.08 mm, slice thickness = 0.46 mm, contour mode = 2, peel mode = 2, inner threshold for

trabecular bone analysis = 395 mg/cm³, cortical mode = 1, and threshold for cortical analysis = 690 mg/cm³.

II.9. Histomorphometric analysis

Mice were treated with RANKL and / or analog 290 for 3 days. At 72 hrs before sacrifice, they were injected with tetracycline (first marker) and at 36 hrs before sacrifice, injected with calcein (second marker). Histomorphometric parameters on proximal metaphyses of left tibiae were measured at the Ito Bone Histomorphometry Institute (Niigata, Japan) and described according to the nomenclature system

II.10. Preparation of SPT and SPT assay

Cell and microsomal fractions containing SPT were prepared from CHO-K1 cells and LY-B cells (as a negative control of SPT activity) and mouse tissues, respectively (Merril et al., 1983, Williams et al., 1984)). CHO cells were cultivated in spinner bottles containing 1 liter of ES medium (Nissui Pharmaceutical Co., Tokyo, Japan) supplemented with 2 mM L-Gln, NaHCO₃ (1 g/l), 10 mM Hepes-NaOH (pH 7.4) and 5 % (v/v) FBS at 37⁰C. The membranous fraction was prepared essentially as described previously. The presence of SPT was monitored by Western blotting using an anti-serine palmitoyltransferase antibody (Cayman Chemical, MI, USA). For mouse tissues, mice were killed by decapitation, and liver, kidney and lung were removed, minced with scissors, and homogenized with a glass

homogenizer under isotonic conditions with Hepes (pH7.4), sucrose and EDTA. A microsomal pellet was prepared by serial centrifugation, suspended in 1 ml/g of tissue with 50 mM Hepes (pH 7.4), 5 mM EDTA, 5 mM DTT and 20%(w/v) glycerol, and stored at -80°C (Hanada et al., 2000).

Either the cell or microsomal fraction containing SPT was incubated in 200 µl of a standard SPT reaction buffer (50 mM Hepes-NaOH buffer (pH 7.5) containing 5 mM EDTA, 5 mM dithiothreitol, 50 µM pyridoxal phosphate, 25 µM palmitoylCoA, and 0.1 mM L-Ser at 37°C for 10 min. To label the product, either L-[³H]Ser (50 mCi/mmol: Amersham Pharmacia Biotech, NJ, USA) or [¹⁴C] palmitoyl-CoA (Amersham Pharmacia Biotech) was used. After the reaction was stopped, lipids were extracted, and the radioactively labeled 3-ketodihydrosphingosine (KDS) was detected and measured as described previously (Merril et al., 1983, Williams et al., 1984).

III. Results

III.1. Screening of amino acids and their derivatives

We reported previously that L-Ser was indispensable for osteoclasts to form *in vitro* (Ogawa et al., 2006). Namely, when L-Ser was depleted from the regular medium, the expression of c-Fos as well as NFAT2 was found to be significantly downregulated in both RAW264 cells and bone marrow macrophages. Conversely, the addition of L-Ser without other NEAA has restored the expression of NFAT2, and the retroviral transfer of NFAT2 appeared to compensate for the depletion of L-Ser (Ogawa et al., 2006). Regarding this, D-Ser was found to be unable to substitute for L-Ser and instead, when D-Ser was added together with L-Ser at up to a thirty-fold excess, there was a suppressive effect on both multinuclear cell formation and NFAT2/c-Fos expression. This inhibitory effect of D-Ser was unique to osteoclastogenesis in that the proliferation of mouse embryonic fibroblasts was little affected.

The above results implied that molecules with antagonistic activity against L-Ser might be useful as a tool for modulating osteoclastogenesis. However, since D-Ser showed some toxicity in preosteoclastic cells, we searched systematically for more effective but less toxic of compounds.

In all, we tested about 100 compounds according to the procedure shown in Figure 9. The compounds could be classified into three groups based on their characteristics at the first

screening step; namely, i) those that could substitute for L-Ser and formed MN cells, ii) those that caused cell death, and iii) those that did not influence cell viability but had a weak effect on TRAP-positive MN cell formation. We then examined the inhibitory activity of the third group in the presence of L-Ser, and identified three substances that fulfilled the criteria; H-L-Ser(OtBu)-OMe HCl, N-CBZ-L-Serine methyl ester, and Z-L-Ser-Gly-OEt (Figure 10). H-L-Ser (OtBu)-OMe HCl (#290) showed the most desirable properties.

As shown in Figure 11, the addition of #290 to the regular differentiation system caused significant suppression of TRAP-positive MN cell formation.

III.1.a. #290 inhibited osteoclastogenesis in a dose-dependent manner

To determine whether the addition of #290 correlates with the number of mature osteoclasts, serial doses of #290 were added to the culture medium. First, the RAW264 cell lines were used. #290 was added at 0.1mM-3mM 24 hours before RANKL. TRAP-positive cells were evaluated 96 hours after the RANKL treatment. As shown in Figure 11A, the inhibition by #290 was dose dependent with the almost complete ablation of osteoclastic formation at 3 mM. From this result, I conducted an experiment using these concentrations to analyze the effect of the #290. To confirm the result, I used primary cells, bone marrow macrophages cells (BMM). As shown in Figure 11B, in BMM as well as in RAW264 cells, #290 inhibited osteoclastogenesis in a dose-dependent manner and at and 3 mM did so without

affecting cell viability.

III.1.b.#290 downregulated RANKL/RANK signaling cascade

RANKL is known to activate a signaling cascade leading to the induction of NFAT2 expression/activity, and MAPK and c-Fos play essential roles in this cascade (Tanaka et al., 2005). Actually, depletion of L-Ser was found to cause downregulation of this cascade (Ogawa et al., 2006). Therefore, to investigate whether #290 inhibits osteoclastogenesis through the RANKL/RANK signaling pathway, first, I evaluated the effect of #290 on the activation of MAPK, ERK1/2 and p38. I used RAW264 cells, as shown in Figure 12A. In RAW264 cells, phosphorylation of ERK1/2 was upregulated 15 minutes after RANKL treatment and decreased after 30 minutes. In the 290-treated cells, the activation of ERK1/2 was unchanged. In contrast, the activation and phosphorylation of p38 in normal medium were upregulated 5 minutes after RANKL treatment, and decreased after 15 minutes. In #290-treated cells, the phosphorylation of p38 was downregulated.

Next, I confirmed using BMM as shown in Figure 12B, that the phosphorylation of ERK1/2 and p38 was upregulated 5 minutes after RANKL treatment and decreased after 15 minutes. In #290-treated cells, the phosphorylation of ERK1/2 and p38 was downregulated-signaling cascade under similar conditions caused by L-Ser's depletion.

I then examined their effect on c-Fos and NFAT2 expression using RAW264 cells.

The expression of c-Fos and NFAT2 was detected 24-48 hours after the RANKL treatment. When 3 mM of #290 were included in the regular differentiation reaction, the levels of c-Fos and NFAT2 were found to be significantly reduced as shown in Figure 13. I also confirmed the downregulation of NFAT2 expression using 2 targets of NFAT2 that is CCR1 and HB-EGF, by RT-PCR. Both were downregulated by #290 as shown in Figure 14, suggesting that #290 function by suppressing the RANKL/RANK

Furthermore, I examined the effect of #290 on RANK expression in RAW 264 cells. The expression of RANK was analyzed 8 hours after the addition of analog. Serum depleted medium was used as a control. RANK expression in RAW264 cells was abundant, so I could only evaluate it by immunoblotting (Figure 15A). However, in BMM, the expression of RANK was low, so I used immunoprecipitation with the anti-RANK antibody before immunoblotting. The expression of RANK in #290-treated cells was examined in RAW264 cells and BMM. The expression level of RANK appeared to be significantly downregulated in the #290-treated cells as shown in Figure 15B and moreover, its localization in membrane lipid rafts appeared to be significantly reduced (Figure 15C). Together, the addition of the #290 seemed to suppress the expression of RANK, and it is conceivable that this downregulation causes the suppression of the downstream signaling machinery.

III.2. Analysis of the function of #290 in L-Ser metabolism

III.2.a. L-Ser metabolism is important for osteoclastogenesis

To understand the functional mechanism of the #290, we focused on the metabolism of L-Ser. L-Ser is known to be converted to ceramide/sphingolipids in mammalian cells through the condensation of serine and palmitoyl CoA by serine palmitoyltransferase (SPT), producing 3-ketodihydrospingosine (KDS). The involvement of this pathway in MN cell formation was confirmed using Myriocin, an SPT inhibitor. When 1.0 μM of Myriocin was added to RAW264 cells in sphingolipid-free medium, the expression of c-Fos and NFAT2 as well as RANK was found to be significantly downregulated (Figure 16), suggesting that L-Ser's metabolism through SPT plays an essential role in the activation of the RANKL/RANK signaling cascade. Since L-Ser was present in the medium, the results also suggested that L-Ser *per se* does not act directly. Moreover, when FB1, an inhibitor of ceramide synthase in the salvage pathway of ceramide synthesis, was used, it had a similar effect on c-Fos, NFAT2 and RANK to myriocin (Figure 16).

Furthermore, on the addition of LacCer to #290-treated cells, the formation of TRAP-positive MN cells and the expression of NFAT2 and c-Fos recovered. (Figure 17)

III.2.b. #290 inhibits SPT activity

To confirm the involvement of SPT as a target of the #290 more directly, I prepared the

fraction contain SPT and examined the effects of #290 on the formation of KDS.

In the SPT assay, SPT catalyzes the condensation between L-Ser and palmitoyl CoA. So I first I isolated SPT from SPT source, CHO-K1 cells. According to Hanada *et al.*, I isolated SPT from the CHO-K1 cell membrane and used LY-B cells as a negative control. LY-B cells are a mutant form of CHO-K1 cells that do not express SPT because they lacking of LCB1 subunit. To identify SPT, I used an anti-SPT antibody that recognized the LCB2 subunit. LCB2 was identified at 58 kDa, as shown in Figure 18. Then I purified SPT from the cell membrane and obtained a band at 58 kDa as shown in Figure 18C.

I used this SPT for the assay according to Williams *et al.*, and [³H]L-Ser as a substrate for SPT. L-Ser will condensate with palmitoyl CoA in a reaction catalyzed by SPT to produce 3-KDS. Because I labeled L-Ser with [³H], I hoped to detect it on TLC plate. Unfortunately, I could not identify 3-ketodehydrospinganine (KDS). This is probably because inactivation of the SPT enzyme occurred during the purification step.

Next, I tried to isolate a microsomal SPT from HEK 293 cells and mouse tissues such as liver, kidney, lung and spleen. The results are shown in Figure 19A. The migration and pattern of bands are not the same for each of the cells and tissues and the expression of SPT was high in HEK 293 cells. Then, I used all these SPTs for the assay, as shown in Fig. 19B. The product of SPT was detected at RF=0.7 and I identified this band as 3-KDS. The most products were found in the microsomal SPT from the liver. Therefore, according to this

result, I used microsomal SPT from the liver to evaluate the effect of the #290 on 3-KDS production.

Next, I used the microsomal SPT from liver to evaluate the effect of the #290 on 3-KDS production. The previous result showed that [³H]KDS is very weak and needs a very long exposure to be detected in TLC. Therefore, I changed the labeled-substrate to [¹⁴C]-palmitoyl CoA.

As shown in Figure 20, we measured the production of 3-KDS using [¹⁴C]-palmitoyl CoA as a substrate. When 1 mM L-Ser was included in the reaction mixture containing the microsomal fraction of mouse liver, the production of KDS was clearly observed, in contrast to that from LY-B cells which are known to lack SPT activity (Hanada et al, 2000). Both D-Ser not #290 produced KDS and when five-fold excess of D-Ser and #290 was added together with L-Ser, the production of KDS was reduced to 20% and 75% of the control reaction, respectively (Figure 20) Since D-Ser was reported to inhibit KDS production in a competitive manner, #290 seemed to function by competing with L-Ser. Together, these results strongly suggested that the metabolite, in particular ceramide and its derivatives, play a role in the activation of the RANKL/RANK signaling cascade through the modulation of RANK expression and that #290 functions at SPT reducing the metabolism L-ser.

III.3. *in vivo* experiments using normal and osteoporotic model mice

The above studies showed the potential of the #290 as an inhibitor of osteoclastogenesis *in vitro*. I then wanted to examine its effect *in vivo*, aiming to obtain answers to two questions; namely, does the #290 actually suppress osteoclastic formation *in vivo* and does the #290 modulate bone turnover? To this end, I used normal mice and osteoporotic-model mice.

For osteoporotic-model mice, I prepared mice whose bone turnover was enhanced by introducing a recombinant RANKL by intraperitoneal injection. This procedure was previously reported as useful for studying the consequences of high bone turnover for bone quality and strength in animals (Stolina et al., 2008).

III.3.a. LD50 test of #290

I examined the acute toxicity of #290 to know the toxic dose of this substance. Animals were treated with substances after at least 5 days of adaptation. They were observed frequently on the day of treatment during normal working hours and the nature and time of all adverse effects were noted. Where any animals died, the time of death was noted, during the 1st day in hours and thereafter in days. Observations and weighing were carried on for 14 days and the experiment was then terminated. If no recovery was noted during this period or if late deaths occurred, the period of observation was extended until the body weight of the surviving animals increased clearly. The experiment was then considered completed. All

surviving animals were sacrificed at the end of each test, autopsied, and examined macroscopically for any pathological changes. The LD₅₀ of #290 on C57BL6 mice was examined first: at 1600 mg/kgBW 25 % of the population died, while at 2900 mg/kgBW and 5000 mg/kgBW, caused 80 % died. From calculations described before, the LD50 was 128mM (Figure 21).

III.3.b. Effects of #290 on normal mice

Mice were administered by #290 16.7 mg/kgBW twice a day for 1 month to 3 months. Isolated tibia then analyzed by pQCT and histomorphometry as shown in figure 22 and 23. The administration for 3 months in C57BL6 mice apparently caused no significant effect on condition such as body weight(data not shown), while bone density remained high (Figure 22).

Further, the effects of #290 on the formation of osteoclasts was measured using microCT and histomorphometry, and a significant different was identified (Figure 23 and 26).

III.3.c. Preparation of osteoporotic-model mice

JM109/pGEX-2TK-RANKL was used to produce a recombinant RANKL. After its isolation and identification, the r-RANKL was diluted with PBS and stored as an aliquot at -80°C.

To evaluate the effect of r-RANKL to induce osteoporotic mice, I used serial doses of r-RANKL ranging from 0.8 $\mu\text{g}/\text{mouse}$ to 100 $\mu\text{g}/\text{mouse}$. r-RANKL was administered by intra-peritoneal injection for three days and then on day four, the mice were sacrificed by cervical dislocation and the tibiae were isolated for a pQCT examination.

The administration of 100 μg of RANKL per day for three days in C57BL/6 mice was found to induce a loss of bone density in trabecular bone of the tibia as shown in Figure 24, when assessed using pQCT. The density in cortical bone, on the other hand, was unaffected under the conditions.

III.3.d. Effects of #290 on osteoporotic-model mice

I then examined the effect of the #290 using osteoporotic-model mice as well as untreated C57BL6 mice, and examined the dosage effect of #290 on bone turnover in terms of bone density (Figure 25). When 16.7 mg/KgBW of #290 was administered into untreated mice for 3 days, a significant increase in bone density was observed (Figure 25A), suggesting an apparent effect of #290 on bone resorption. Subsequently, we tested its effect in RANKL-treated mice, and when #290 was administered twice a day prior to the RANKL treatment and the following 4 days at three different concentrations, the loss of bone density in trabecular bone of the tibiae was significantly blocked (Figure 25).

IV. Discussion

Previous findings that the presence of L-Ser was required in the *in vitro* differentiation system and that the introduction of D-Ser suppressed the formation of the osteoclasts suggested a novel method of regulating osteoclastogenesis, and prompted us to search for compound(s) with more desirable properties. We consequently identified three compounds that fulfilled the conditions. Regarding these molecules, common structure in the three substances is only that they contain L-Ser backbone and form methyl/ethyl ester, and yet we have been unable to identify the structural characteristic discriminating the three molecules from the rest. Therefore, at this moment, we cannot predict the desired molecules solely from the standpoint of structure. Of these molecules, I focused on one of them #290 (H-L-Ser[OtBu]-OMe HCl) in this study owing to its water-solubility and relatively high inhibitory activity; it showed not only an inhibitory activity in osteoclastogenesis *in vitro*, but significant and rapid suppressive effect on bone turnover in mice.

Another characteristic feature of #290 was that it showed a competitive effect with L-Ser on SPT that catalyzes condensation of palmitoyl coenzyme A and L-Ser to produce 3-ketodihydrosphingosine (KDS). D-Ser was reported to inhibit KDS production in a competitive manner (Hanada et al., 2000). Incubation of SPT with [palmitoyl 1-¹⁴C] palmitoyl CoA and #290 did not produce [¹⁴C] KDS. An analysis of the production of KDS from L-Ser was performed using partially purified SPT and [¹⁴C]-palmitoyl CoA revealed the

analog to be ~50% as effective as D-Ser, suggesting that #290 has a weaker activity than D-Ser as an inhibitor of SPT. Combined with the results obtained using a SPT inhibitor Myriocin, these results therefore strongly suggest that the analog exerts the effect by downregulating the production of the starting metabolite of L-Ser metabolism by SPT, and this may be the cause of inhibitory activity of osteoclastogenesis. Hanada *et al.* reported that all of the amino, carboxyl and hydroxyl groups of L-Ser are responsible for the substrate to regulation of SPT (Hanada et al., 2000a). Since only the amino group is conserved intact in the #290, the weaker activity observed in the #290 could be due to lacking both carboxyl and hydroxyl groups at their appropriate positions. Furthermore, D-Ser showed toxic effect in differentiating RAW264 cells at 3mM, whereas the same administration showed little effect on fibroblastic cells, suggesting that high turnover of serine metabolism might be prerequisite characteristic to osteoclastogenesis.

I observed that the #290 treatment caused the reduction of RANK expression and the relocation of RANK from membrane rafts. This maybe explained the down-regulation of MAPK activity and the expression level of c-Fos and NFAT2 in those cells. The expression of RANK was also significantly suppressed by 1.0 μ M myriocin administration. Therefore, it seems that reduced sphingolipids metabolites caused by down-regulation of SPT activity by #290 resulted in the down-regulation of RANK expression level and the modulation of its localization in membrane rafts. Regarding this, glycosphingolipid was reported to play an

important role in osteoclastogenesis (Kitatani et al., 2008, Iwamoto et al., 2001). D-threo-1-phenyl-2-decanoylamino-3-morpholino-1-propanol, a glycosylceramide synthase inhibitor, was shown to completely inhibit the formation of osteoclasts among bone marrow cells and the addition of LacCer rescued the formation of TRAP-positive mononucleated cells but not multinucleated cells. Here the addition of LacCer to #290-treated RAW264 cells rescued the suppressed formation of TRAP-positive MN cells accompanying an up-regulation of NFAT2 expression. Therefore, the recovery obtained with LacCer observed in this study may reflect either the difference in cell-type used or the partial inhibition of SPT by #290. In any case, how LacCer regulates RANK expression is an intriguing question and awaits further analysis.

Usefulness of #290 as a modulator of osteoclastogenesis was further tested *in vivo*. In fact, we observed the dosage effect of the #290 *in vivo* using control and high bone-turnover mice. Osteoporosis and rheumatoid arthritis are considered major diseases in the field of bone metabolism in terms of number of patients affected as well as the severity of their effect on ordinary life. Various approaches and drugs have been used to treat these diseases. The #290 with an inhibitory activity of SPT thus identified may have unique potential as a therapeutic tool, given that is completely different from currently available drugs in terms of its chemical as well as biological properties and has low production costs. Importantly, since L-Ser is considered as a nonessential amino acid in mammals and the methodology described

below does not modify the L-Ser biosynthetic pathway at genetic level, there should be little damage to the homeostasis. Although treatment for 3 months did not caused any obvious change in mice, a more precise analysis may be needed if the #290 is to be used for therapeutic purpose.

VI. Figures and legends

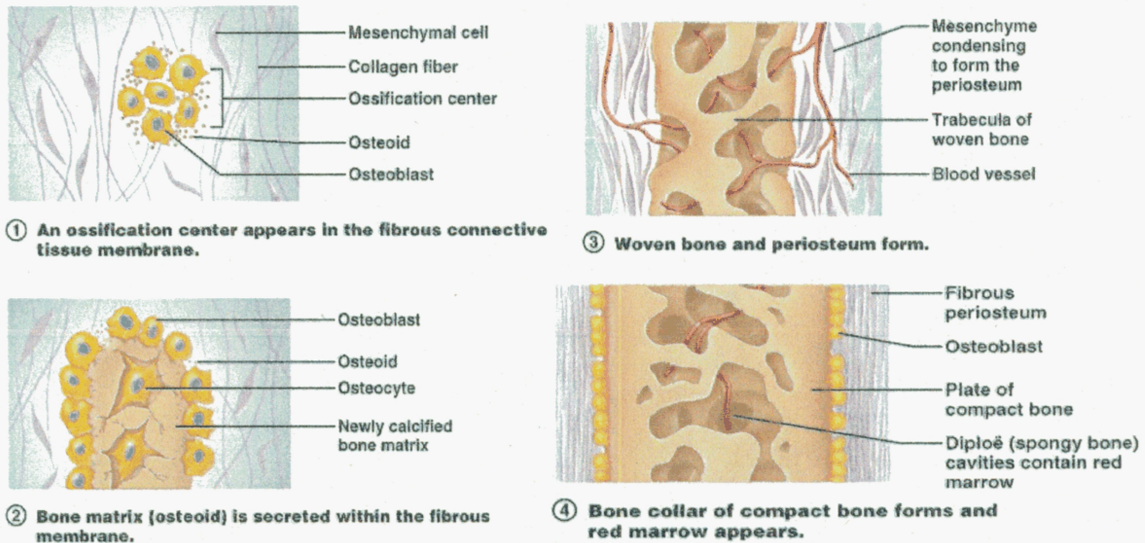


Figure 1. Intramembranous ossification.

An ossification center appears in the fibrous connective tissue membrane (1). Selected centrally located mesenchymal cells cluster and differentiate into osteoblast, forming an ossification center. Bone matrix (osteoid) is secreted within the fibrous membrane (2). Osteoblast begin to secrete osteoid, which is mineralized within a few days, trapped osteoblasts become osteocytes. Woven bone and periosteum bone (3). Accumulating osteoid is laid down between embryonic blood vessels, which form a random network of trabeculae. Bone collar of compact bone forms and red marrow appears (4). Trabeculae just deep to periostenum thicken, forming a woven bone collar that is later replaced with mature lamellar bone. Spongy bone consisting of distinct trabeculae, persists internally and its vascular tissue becomes red marrow.

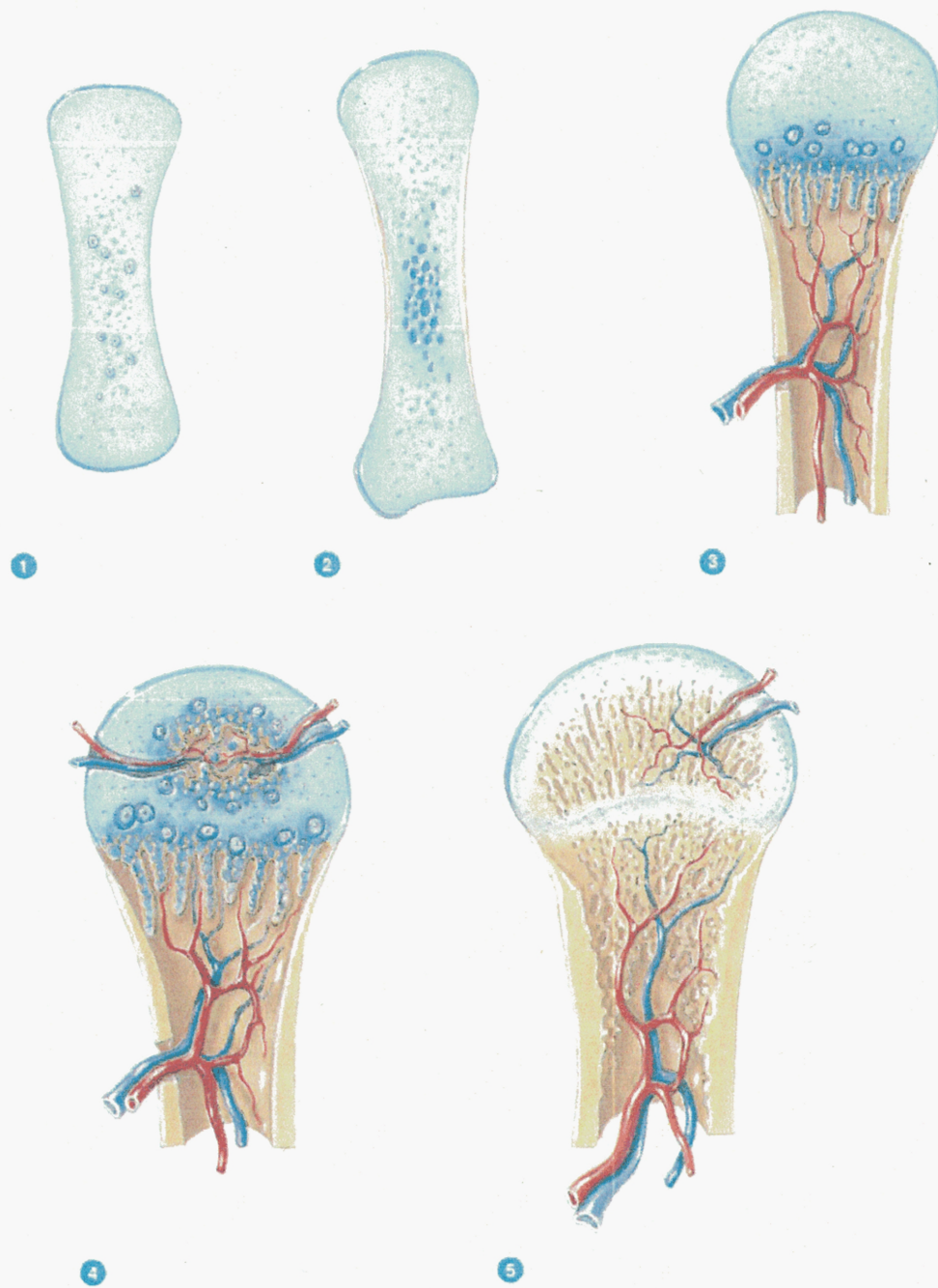


Figure 2. Endochondral ossification.

Chondrocytes at the center of the growing cartilage model enlarge and then die as the matrix calcifies (1). Newly derived osteoblasts cover the shaft of the cartilage in thin layer of bone (2). Blood vessels penetrate the cartilage, new osteoblasts form a primary ossification center (3). The bone of the shaft thickens, and the cartilage near each epiphysis is replaced by shafts of bone (4). Blood vessels invade the epiphyses and osteoblasts from secondary centers of ossification.

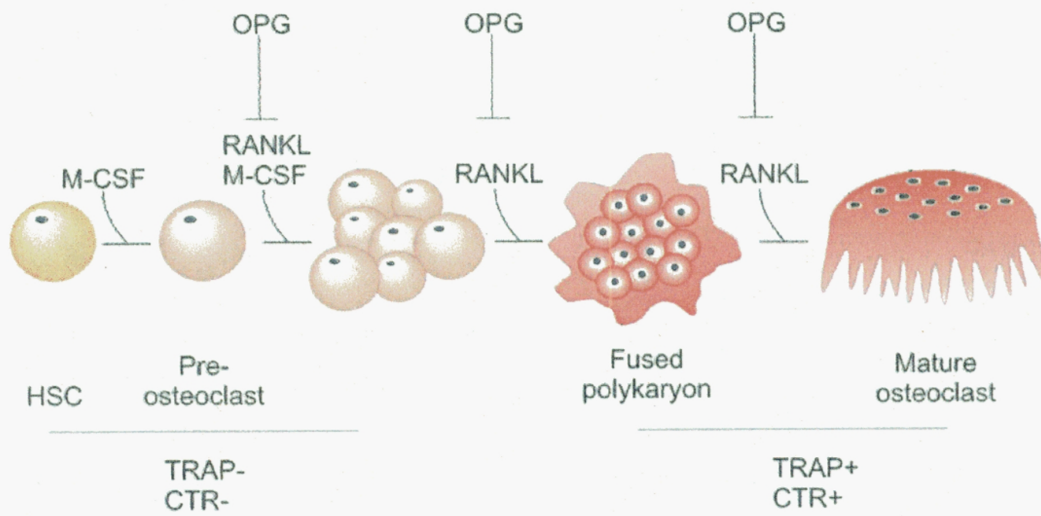


Figure 3. Osteoclastogenesis

The osteoclasts originate from hematopoietic stem cells, which differentiate into osteoclasts through a series of steps involving the commitment of hematopoietic stem cells to the monocyte/macrophage lineage, proliferation of preosteoclasts, and differentiation into mature osteoclasts with resorptive activity.

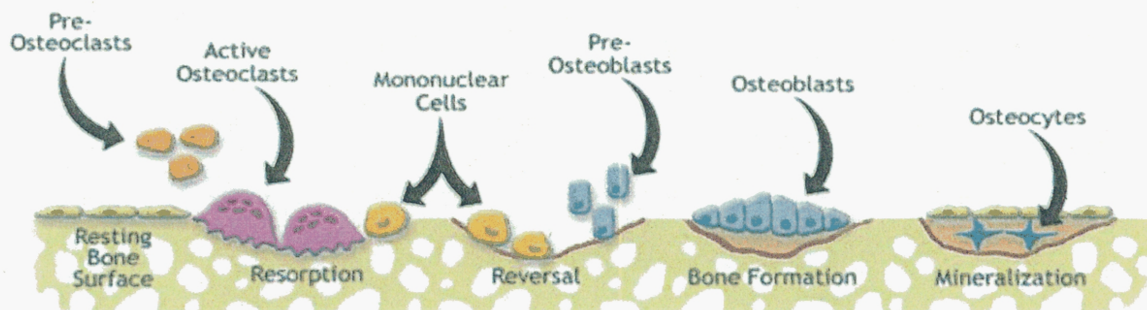


Figure 4. Bone remodeling

Remodeling of bone starts with osteoblastic activation of osteoclast differentiation, fusion, and activation. When resorption lacunae are formed, the osteoclast leaves the area, and mononucleated cells of uncertain origin appear and "clean up" the organic matrix remnants left by the osteoclast. During the resorption process, coupling factors, including IGF-I and TGF- β , are released from the bone extracellular matrix, and these growth factors contribute to the recruitment and activation of osteoblasts to the resorption lacunae. The osteoblasts will then fill the lacunae with new bone, and when the same amount of bone is formed as that being resorbed, the remodeling process is finished, and the mineralized extracellular matrix will be covered by osteoid and a one-cell layer osteoblasts

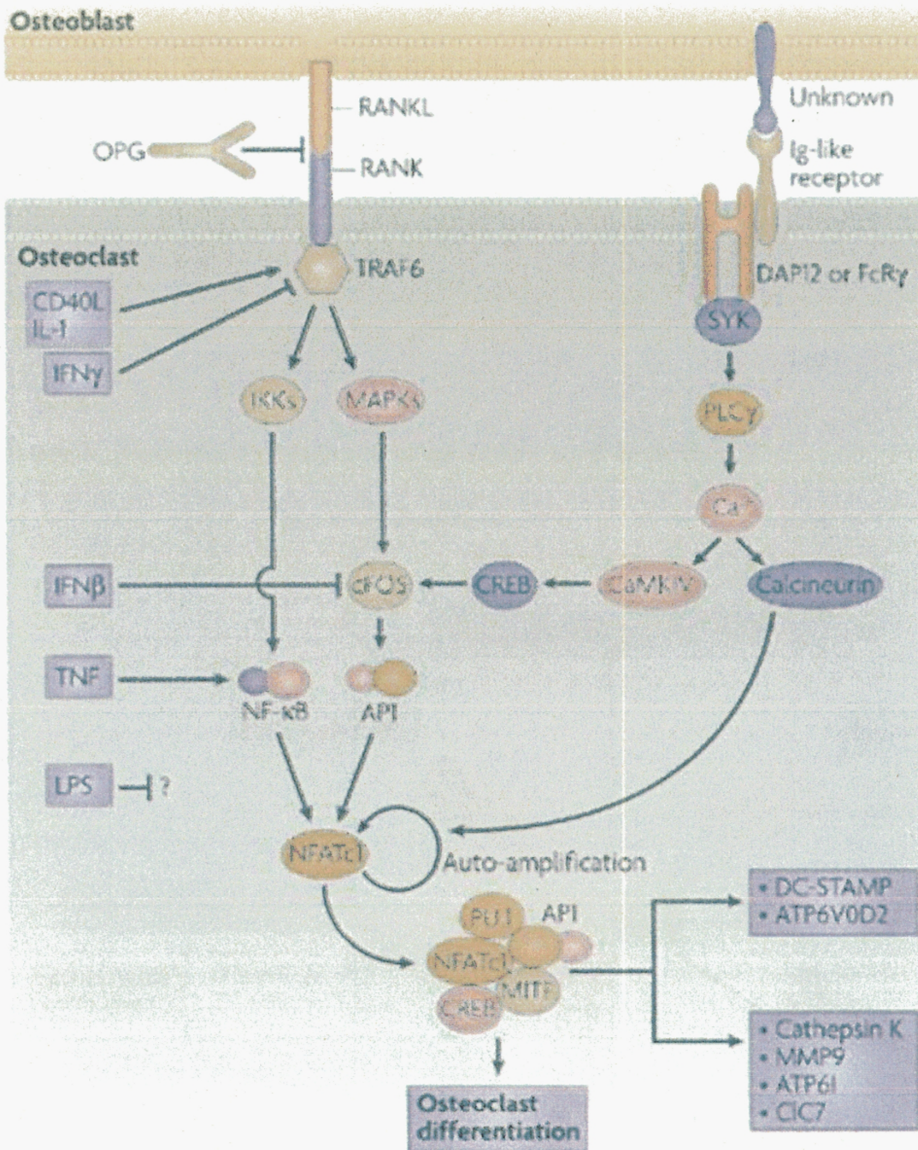
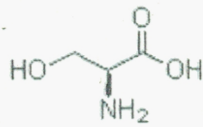
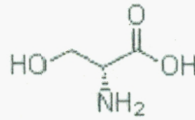


Figure 5. Schematic diagram of the RANKL-RANK-induced signaling cascades that control lineage commitment and activation of osteoclasts (Takayanagi, 2007).



A). L-Serine



B). D-Serine

Figure 6. Molecular structure of L-Serine and D-Serine

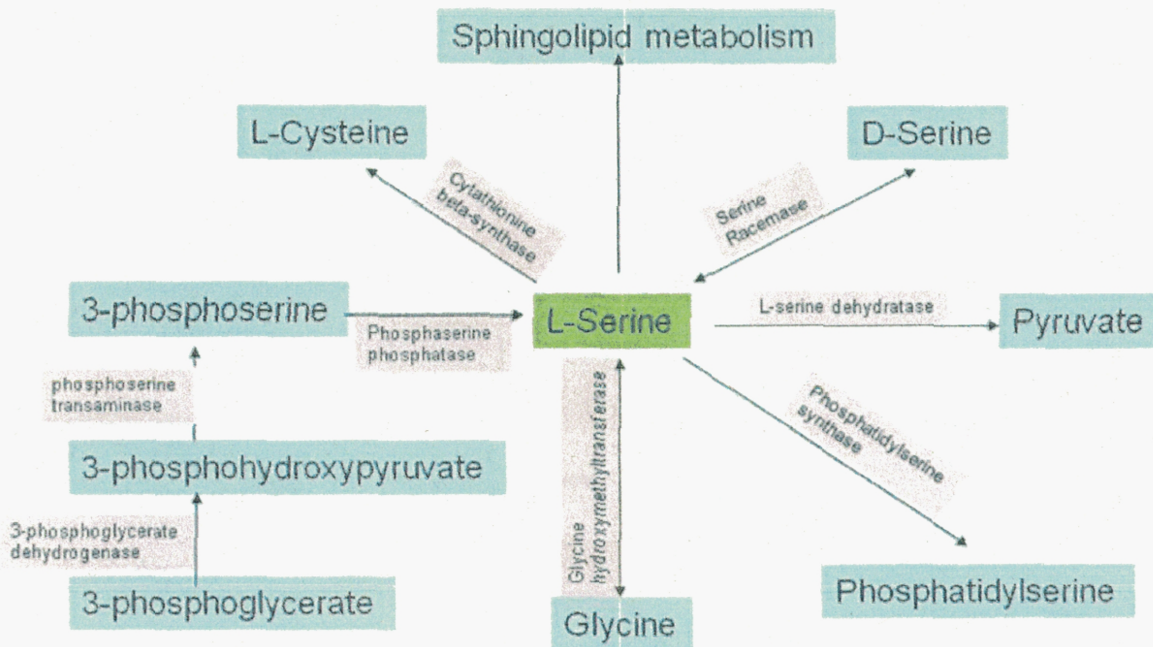


Figure 7. L-Serine metabolism

L-Ser is derived from 3-phospho-D-glycerate, an intermediate of glycolysis and serves as a metabolic precursor/intermediate necessary for various pathways of biosynthesis. These include the production of glycine, L-cystein, phosphatidylserine, sphingolipids, and D-Ser.

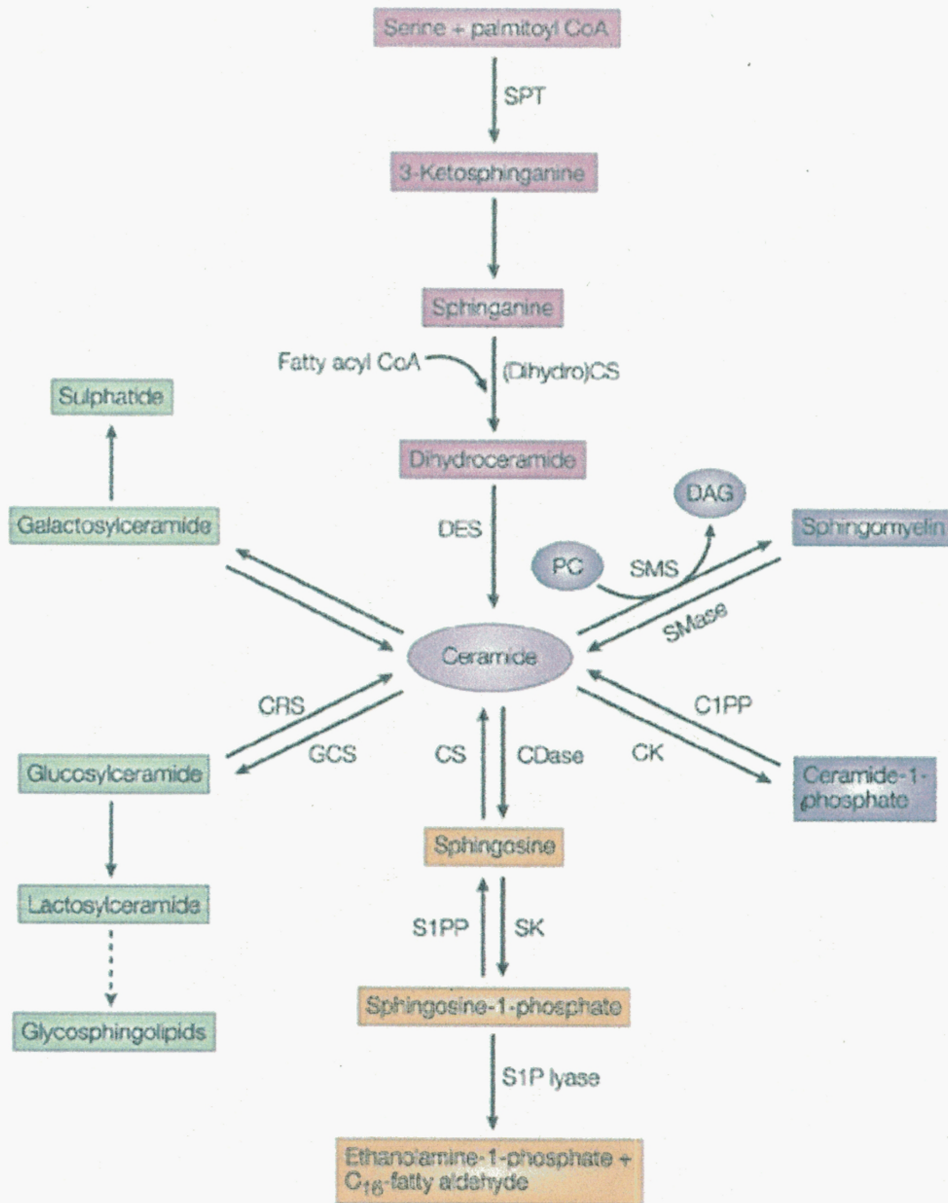


Figure 8. Pathways of sphingolipid metabolism

De novo sphingolipid biosynthesis begins in the endoplasmic reticulum with the condensation of serine and palmitoyl-CoA by serine palmitoyltransferase; 3-ketosphinganine is reduced to sphinganine, which is acylated to dihydroceramides by ceramide synthase or phosphorylated by sphingosine kinase to sphingosine 1-phosphate. The dihydroceramide is desaturated to ceramide and incorporated into sphingomyelin and other complex sphingolipids. Turnover occurs in the plasma membrane, lysosomes, and sphingosine 1-phosphate (Ogretmen and Hannum, 2004)

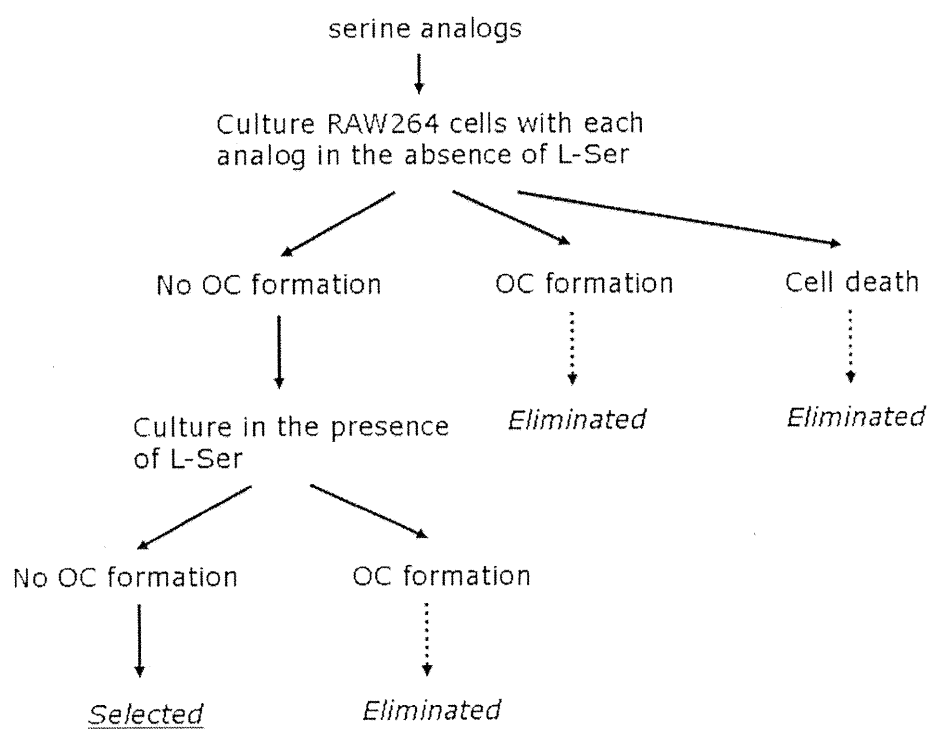


Figure 9. Schematic diagram of the screening of amino acids and their derivatives.

RAW264 cells were cultured under regular conditions in the absence of L-Ser together with 0.1 mM of each substance to be tested for the first screening. Cell morphology was judged after 4 days. Substances that produced few TRAP-positive MN cells were subjected to further screening. At the second screening, RAW264 cells were cultured in the presence of 0.1 mM L-Ser together with various concentrations (0.1-10 mM) of candidate substances, and cell morphology was examined after 4 days.

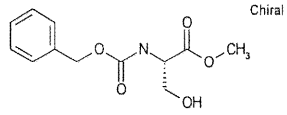
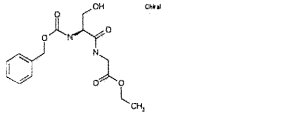
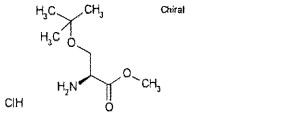
Compounds no.	MOL STRUCTURE	MOL STRUCTURE	MOL NAME
21		C ₁₂ H ₁₅ NO ₅	N-CBZ-L-Serine methyl ester
269		C ₁₅ H ₂₀ N ₂ O ₆	Z-L-Ser-Gly-OEt
290		C ₈ H ₁₈ ClNO ₃	H-L-Ser(OtBu)-OMe HCl

Figure 10. Molecular structures of three compounds identified by the screening strategy shown in Figure 9.

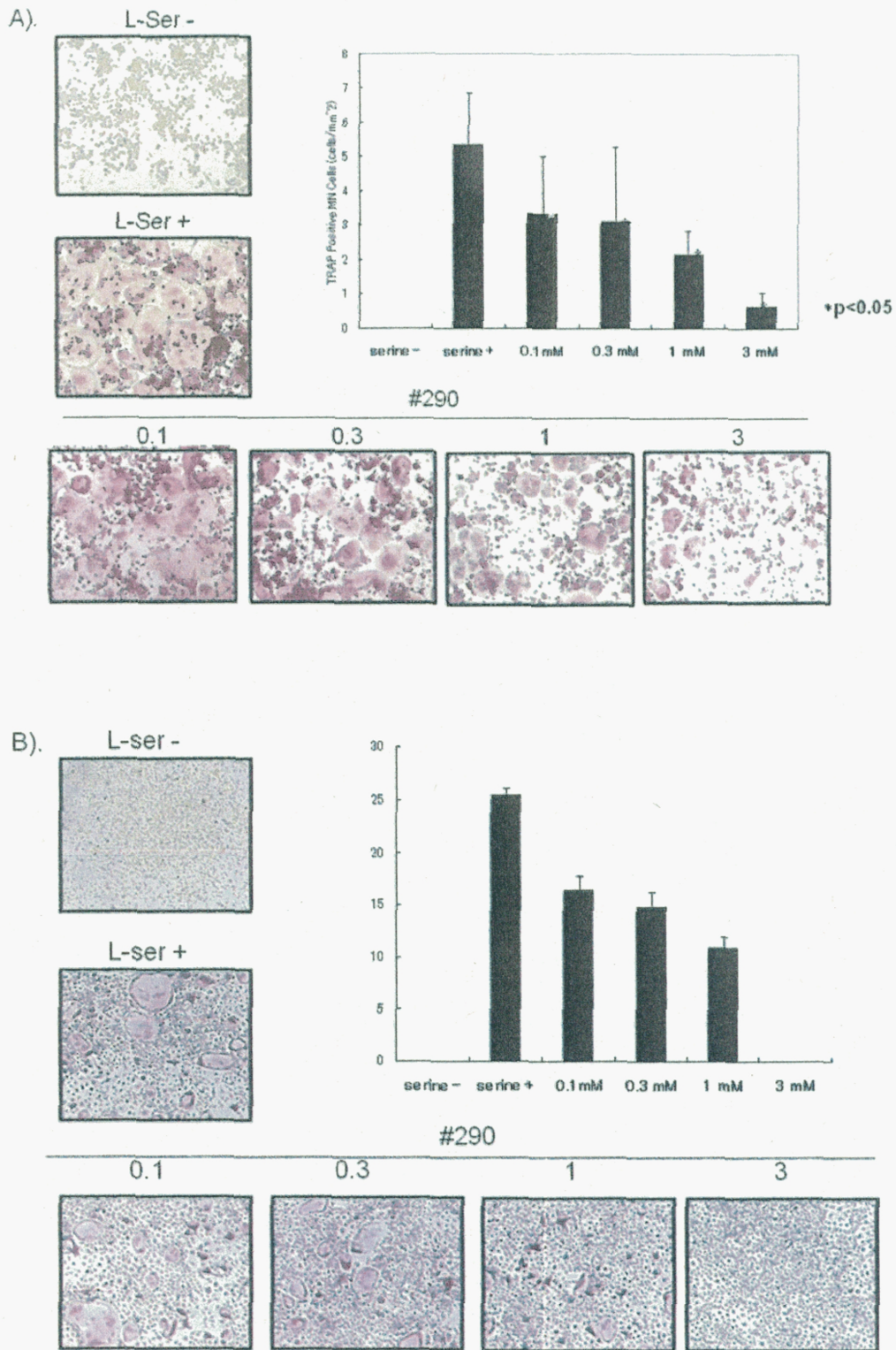


Figure 11. Dose-dependent inhibition of osteoclastic formation by #290

The addition of #290 to RANKL-treated cells resulted in a dose-dependent decrease in the formation of osteoclasts. A) RAW264 cells B) BMM.

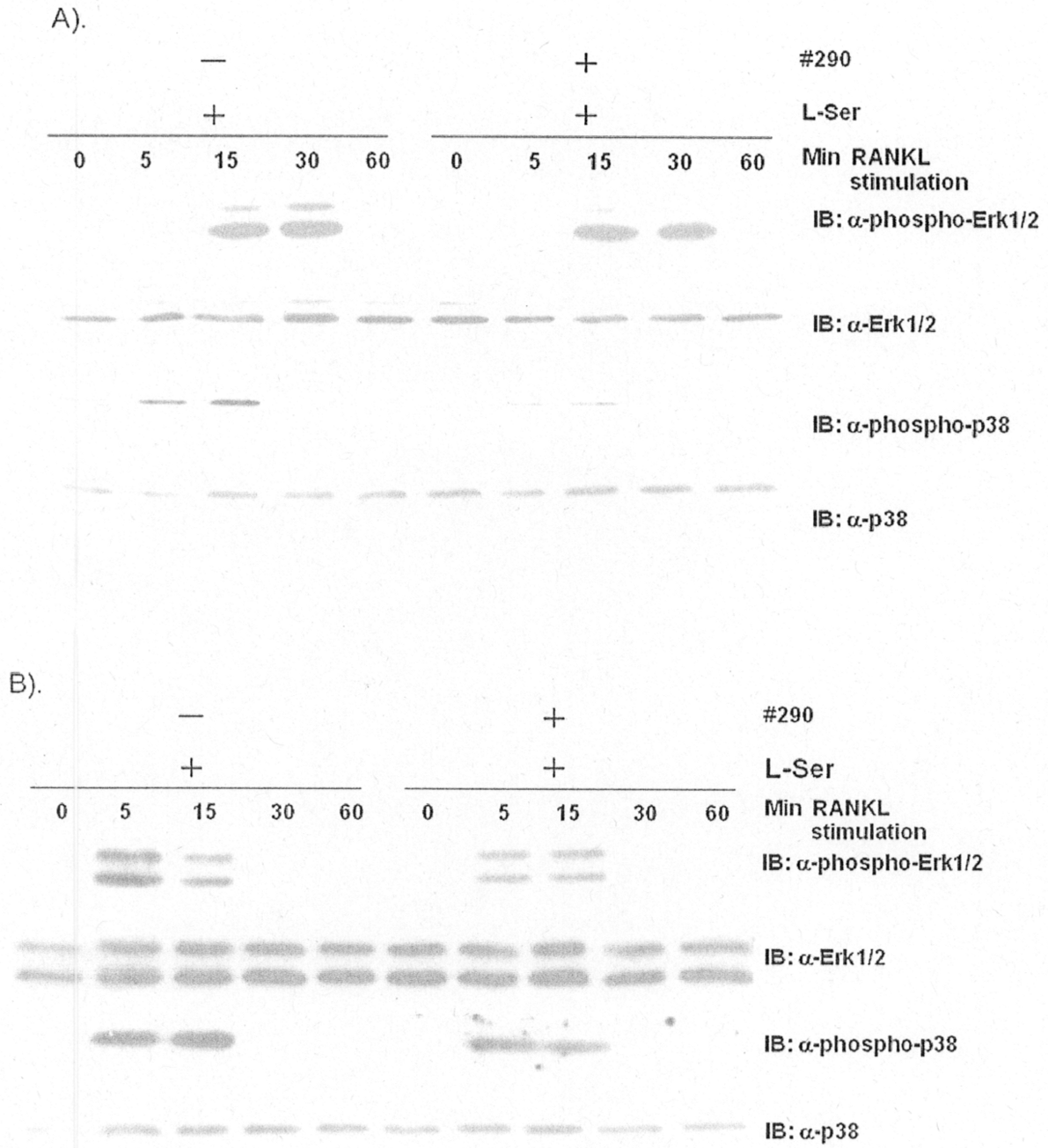


Figure 12. Effects of #290 on MAPK.

Cells were treated with #290, 24 hours before RANKL. Cell lysate was harvest at indicated times and subjected to immunoblotting using anti-NFAT2 and anti-c-Fos antibodies, 1) RAW cells 2) BMM

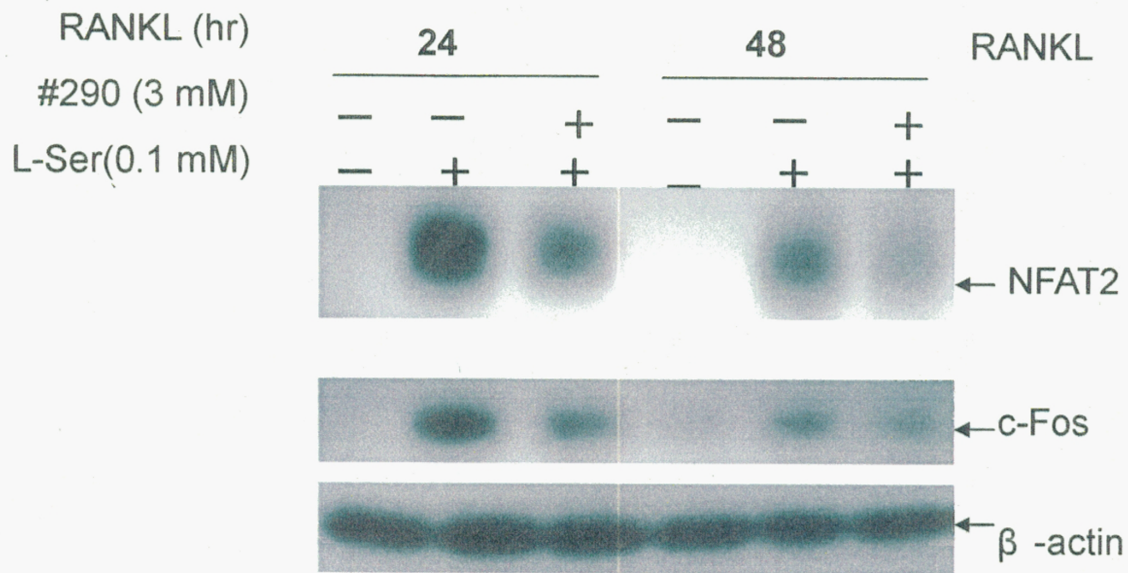


Figure 13. Effects of #290 on c-Fos-NFAT2 expression.

RAW264 cells were treated with #290 24 hours before RANKL, and cell lysate was collected 24 and 48 hours after the RANKL treatment. The expression of c-Fos and NFAT2 was monitored by Western blotting, using anti-Fos and anti-NFAT2 antibody, respectively. Anti- β -actin monoclonal antibody was used for monitoring the amount of protein applied.

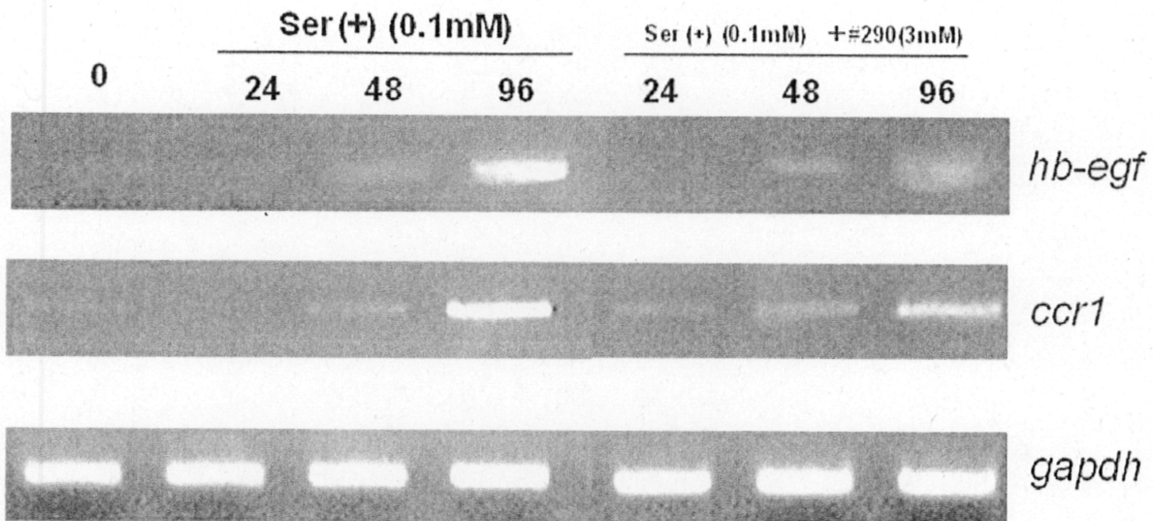


Figure 14. Effects of #290 on the osteoclastogenic gene.

RAW264 cells were treated with #290 24 hours before RANKL treatment and cells were harvested at indicate times and subjected to RT-PCR

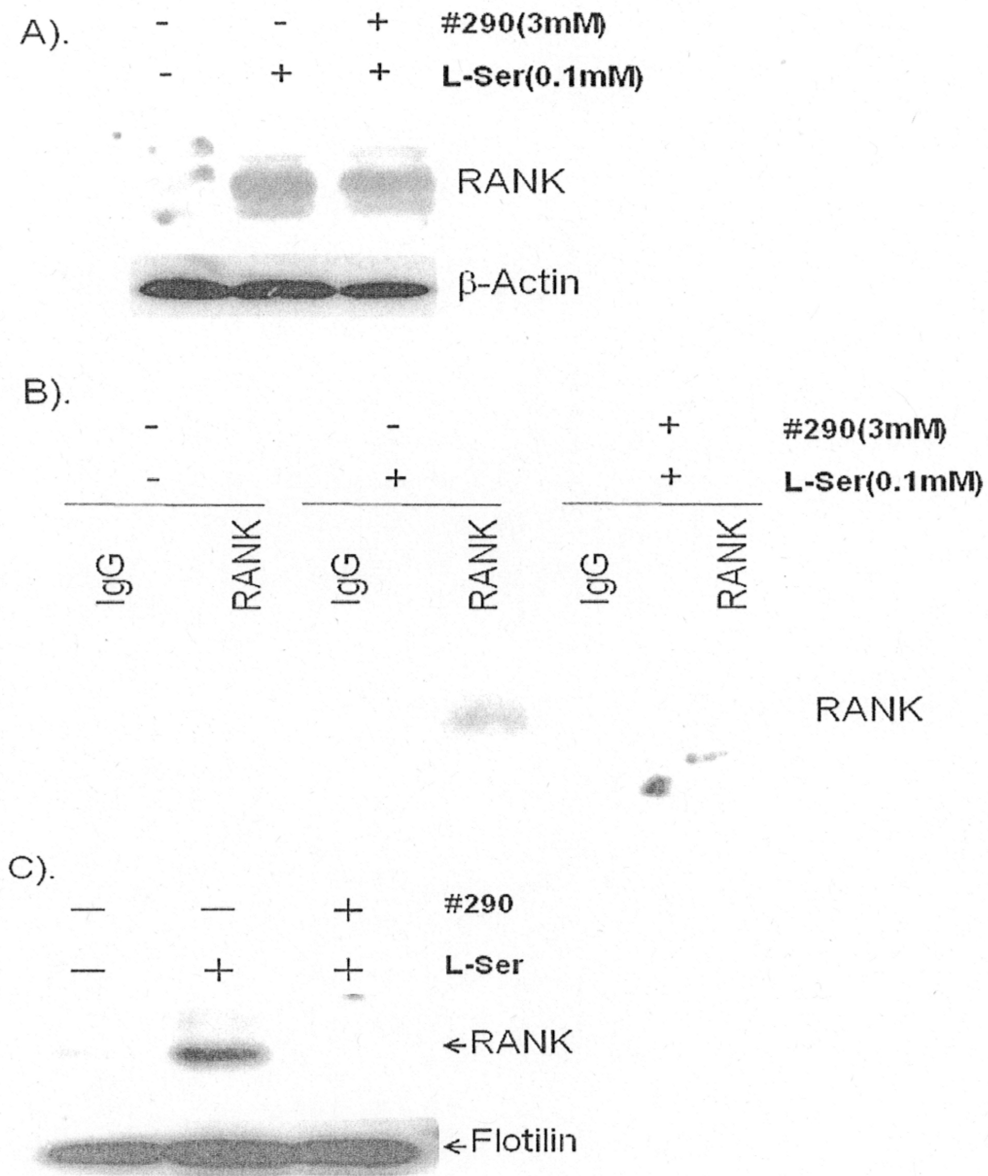


Figure 15. Effects of #290 on RANK expression.

RAW264 cells were cultured in the presence of L-Ser (0.1 mM) and 3 mM of serine analog no. 290. Cell lysates were prepared 24 hrs after the RANKL treatment. Expression of RANK was monitored by Western blotting A). Immunoblotting of RANK in RAW264 cells, B). Immunoprecipitation-Immunoblotting of RANK on BMM C). RANK expression in lipid rafts.

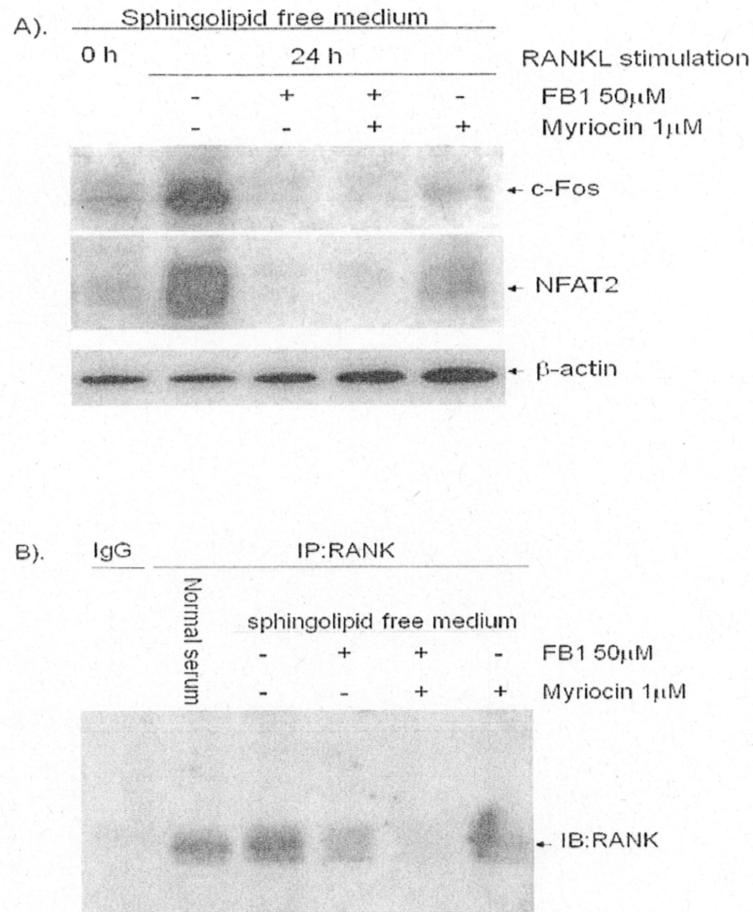


Figure 16. Role of L-Ser metabolism in RANK/RANKL signaling.

A) Effects of myriocin and FB1 on RANK expression. RAW264 cells were cultured under regular conditions using 10% FBS. After 24hrs, the medium was changed to one containing sphingolipid-free serum instead of normal FBS and also either 1 μ M miriocine or 50 μ M FB1, followed by incubation for another 8 hrs. Immunoprecipitation and Western blotting were done as in A). Normal mouse IgG was used as a control. B) Effects of myriocin and FB1 on c-Fos and NFAT2 expression. Cell culturing and the preparation of cell lysates were carried out as in B). Western blotting was then carried out using anti-c-Fos and anti-NFAT2 antibodies.

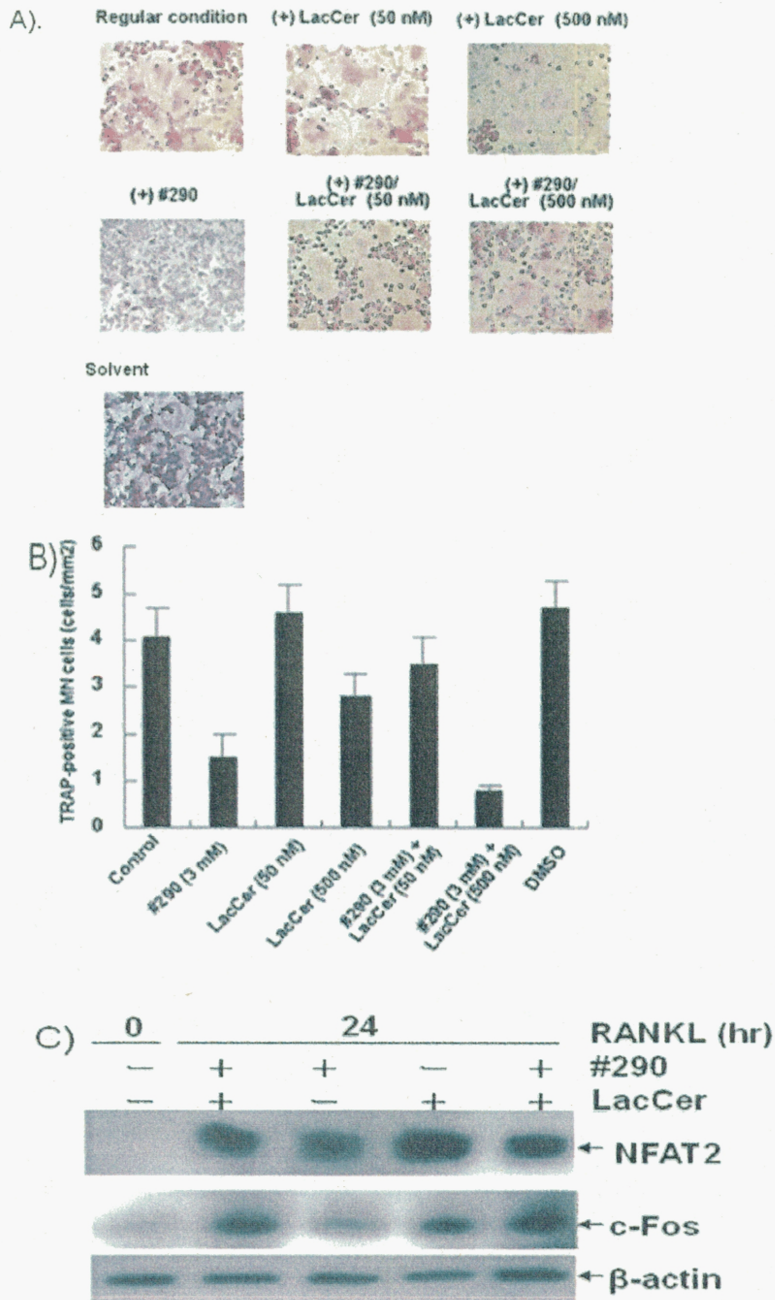


Figure 17. Lactosylceramide rescues the analog-treated cells.

A) When 50 nM Lactosylceramide was added in the *in vitro* differentiation reaction containing 3 mM #290 and incubated for 4 days, the formation of MN cells was found to be recovered to 80% of the normal level. B) The expression of c-Fos and NFAT2 also recovered after Lactosylceramide treatment.

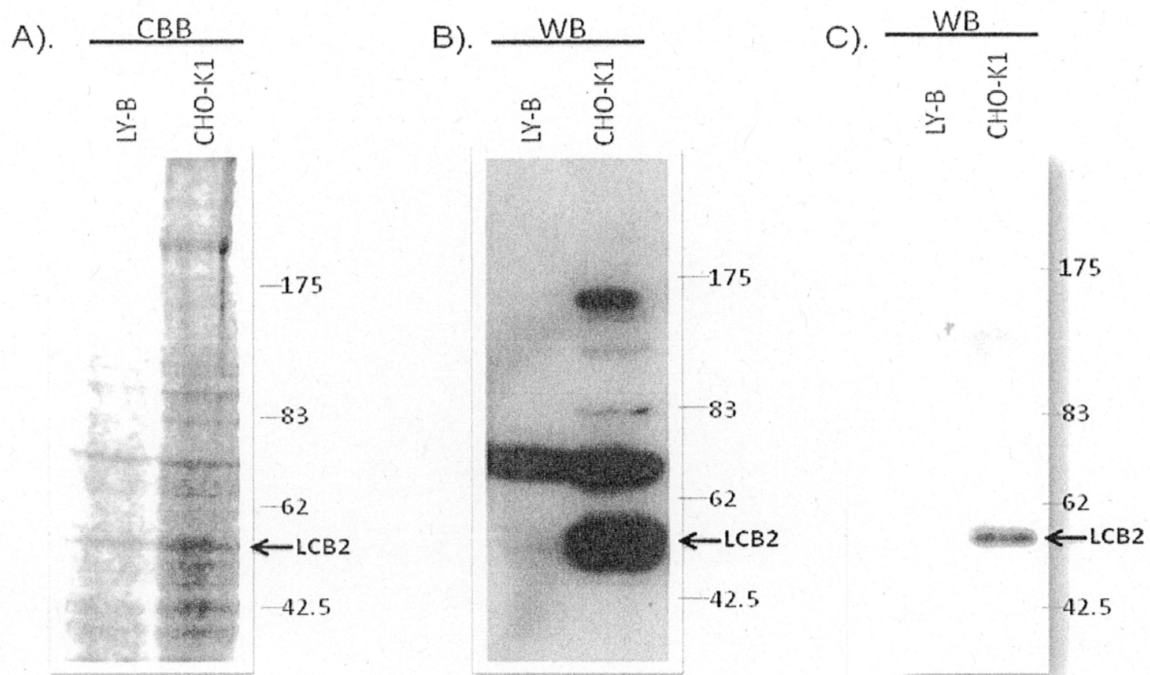


Figure 18. Isolation and identification of SPT from CHO-K1 cells

A). CBB staining of crude extract of CHO-K1 cells and LY-B cells. B). Immunoblotting of crude extract of CHO-K1 and LY-B cells. C). Immunoblotting of fraction containing SPT from CHO-K1 and LY-B cells.

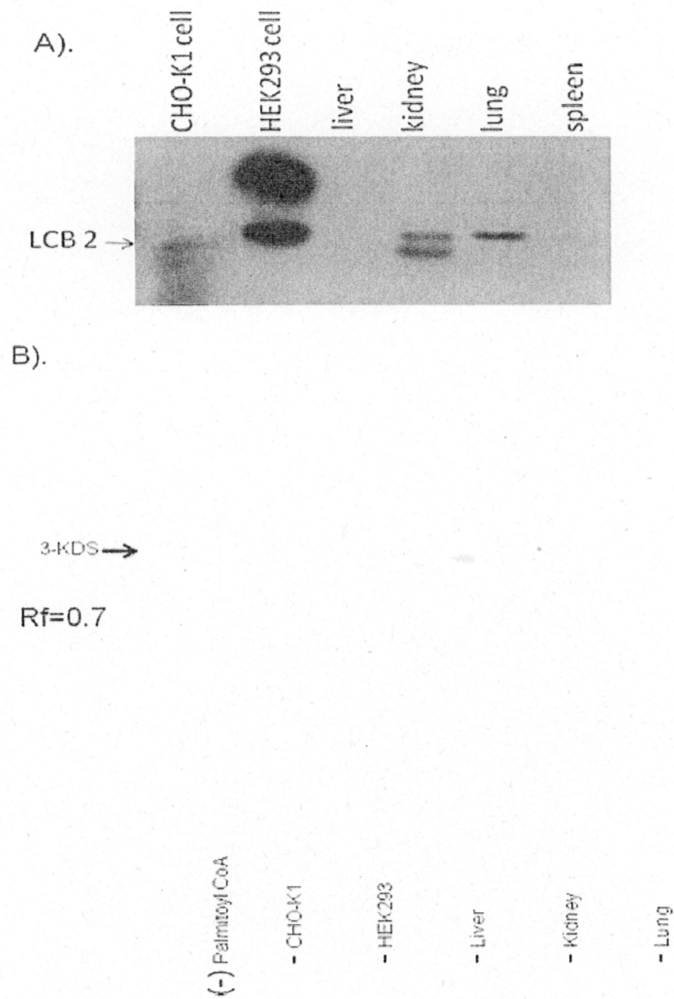


Figure 19. Isolation of SPT from cells and tissues

A). Microsomal fraction was prepared from cells or mouse tissues. Expression of SPT was monitored by Western blotting using anti-SPTB1 antibody. B). SPT assay from SPT of various cells and tissue.

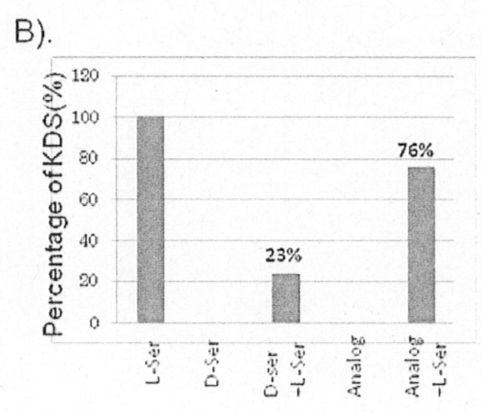
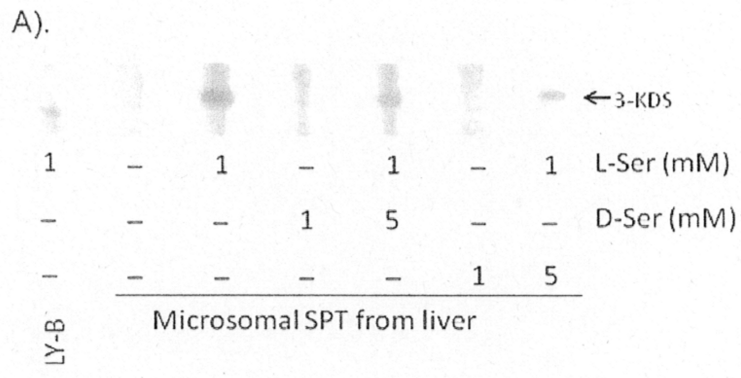


Figure 20. Effects of #290 on SPT activity.

A) Effects of D-Ser and the #290 on production of KDS. The SPT reaction was carried out using partially purified SPT as in A) and [¹⁴C]-palmitoylCoA in the absence or presence of the indicated amount of L-Ser or #290. Production of KDS was detected by thin layer chromatography and quantified using the BASS2500 system. B) Inhibitory mode of the #290

A).

Dose (mg/kgBW)	log dose	no. of mice	no. of dead mice	Probit	Fit
1000	3	5	0	0	1.254918
1600	3.204	5	1	4.33	2.933297
2900	3.462	5	4	5.84	5.055952
5000	3.699	5	4	6.08	7.005833

B).

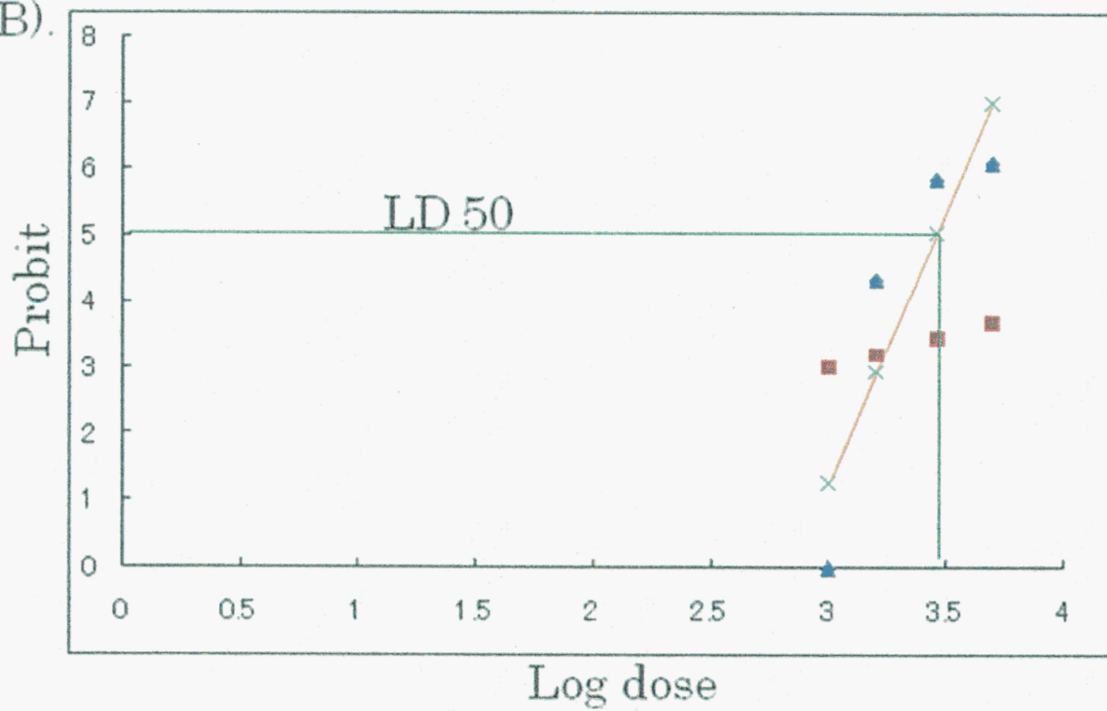


Figure 21. Acute toxicity assay of #290.

A) Indicated amount of #290 was administered intraperitoneal injection into C57BL6 mice and the effect on mortality was assessed after 24 to 2 weeks. B) LD₅₀ was determined as described in “Materials and methods” based on data obtained in A).

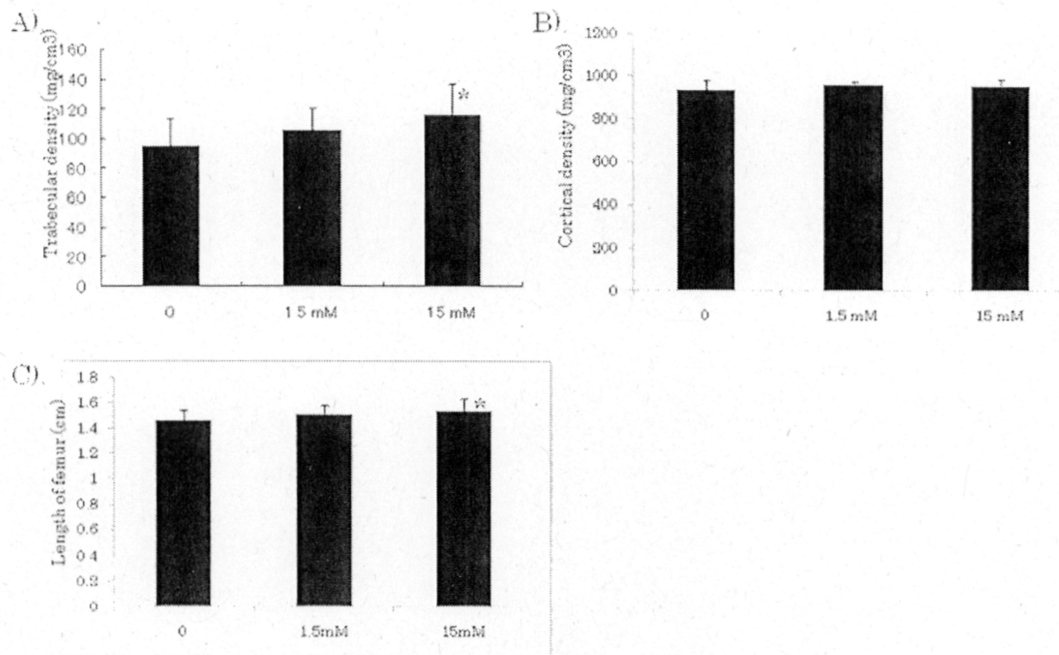


Figure 22. Long-term administration of #290 in mice.

Mice were injected for 90 days with various doses 0-15 mM; bone density and length of femur were measured. A). Trabecular bone B) Cortical bone C). Length of femur

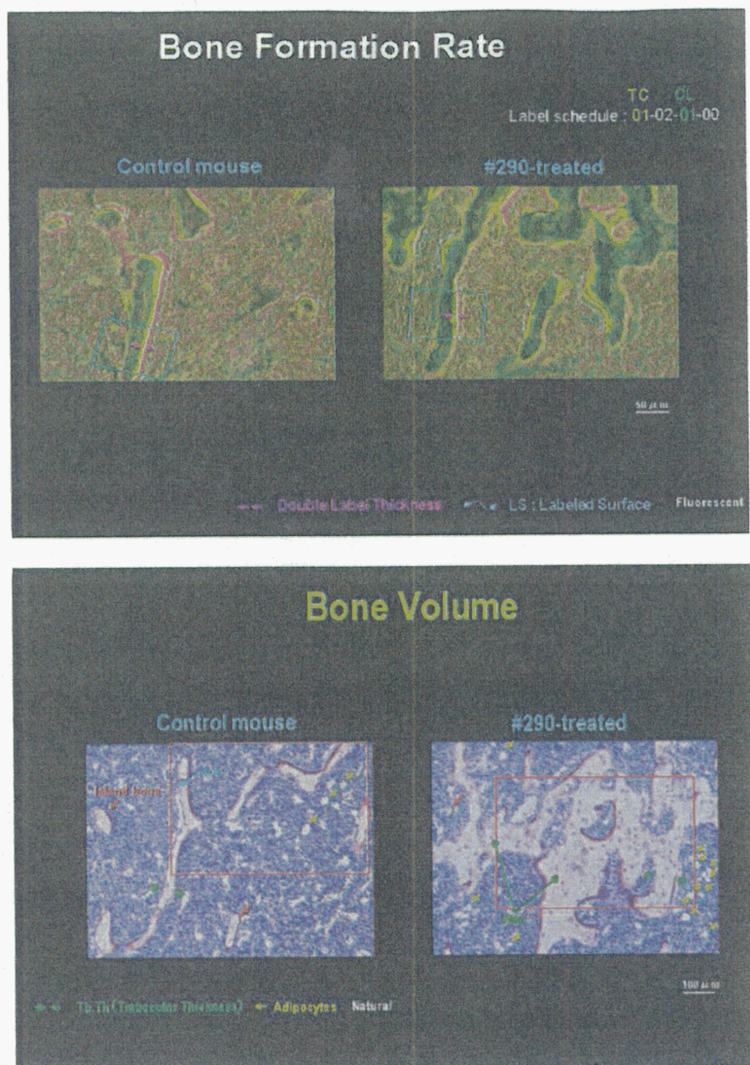


Figure 23. The microscopic images of histomorphometry analysis of tibia. C57BL/6 mice ($n = 6$) were treated with either vehicle or #290 (15 mM) for 4 weeks. During treatment, mice were injected by tetracycline and calcein as marker for calculation growth of rate. A).Bone formation rate B). Bone volume.

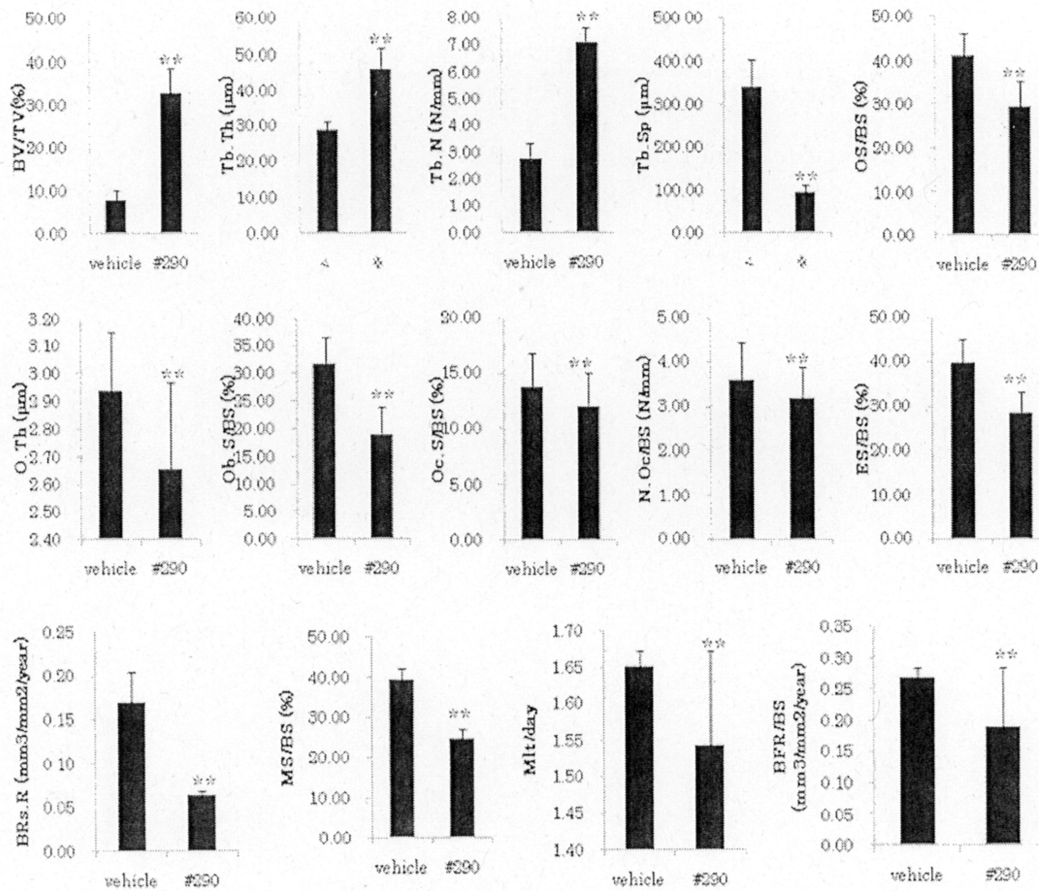
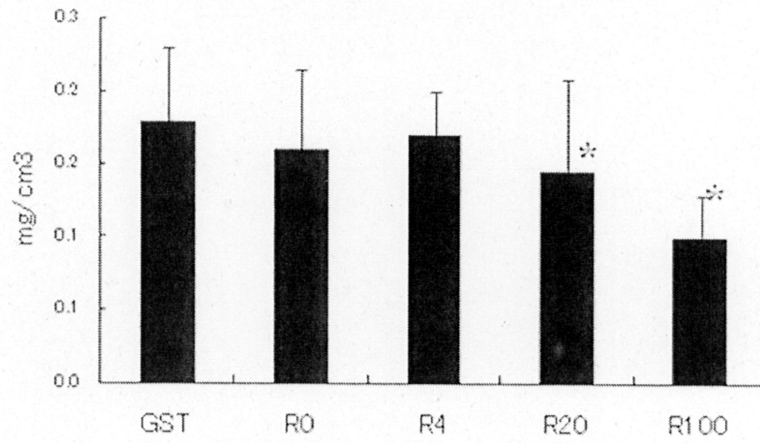


Figure 24. Bone histomorphometry analysis of tibia

C57BL/6 mice ($n = 6$) were treated with either vehicle or #290 (15 mM) for 4 weeks, and left tibiae were used for static and dynamic histomorphometric assay. *BV/TV*, bone volume/tissue volume; *Tb.Th*, trabecular thickness; *Tb.N*, trabecular number; *Tb.Sp*, trabecular separation; *OS/BS*, osteoid surface/bone surface; *O.Th*, osteoid thickness; *Ob.S/BS*, osteoblast surface/bone surface; *Oc.S/BS*, osteoclast surface/bone surface; *N.Oc/BS*, number of osteoclasts/bone surface; *ES/BS*, eroded surface/bone surface; *BRs.R*, bone resorption rate; *MS/BS*, mineralizes surface/bone surface; *Aj.AR*, adjusted apposition rate; *Mlt*, mineralization lag time; *BFR/BS*, bone formation rate/bone surface.

A).



B).

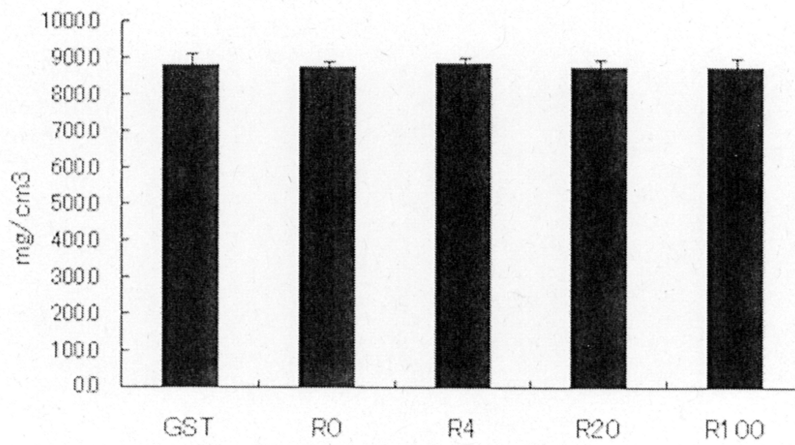


Figure 25. Preparation of high bone-turnover mice.

Indicated amounts of recombinant soluble RANKL was administered to C57BL/6 mouse every day for three days. Bone density was measured as described in "Materials and methods". A) Trabecular density B). Cortical density

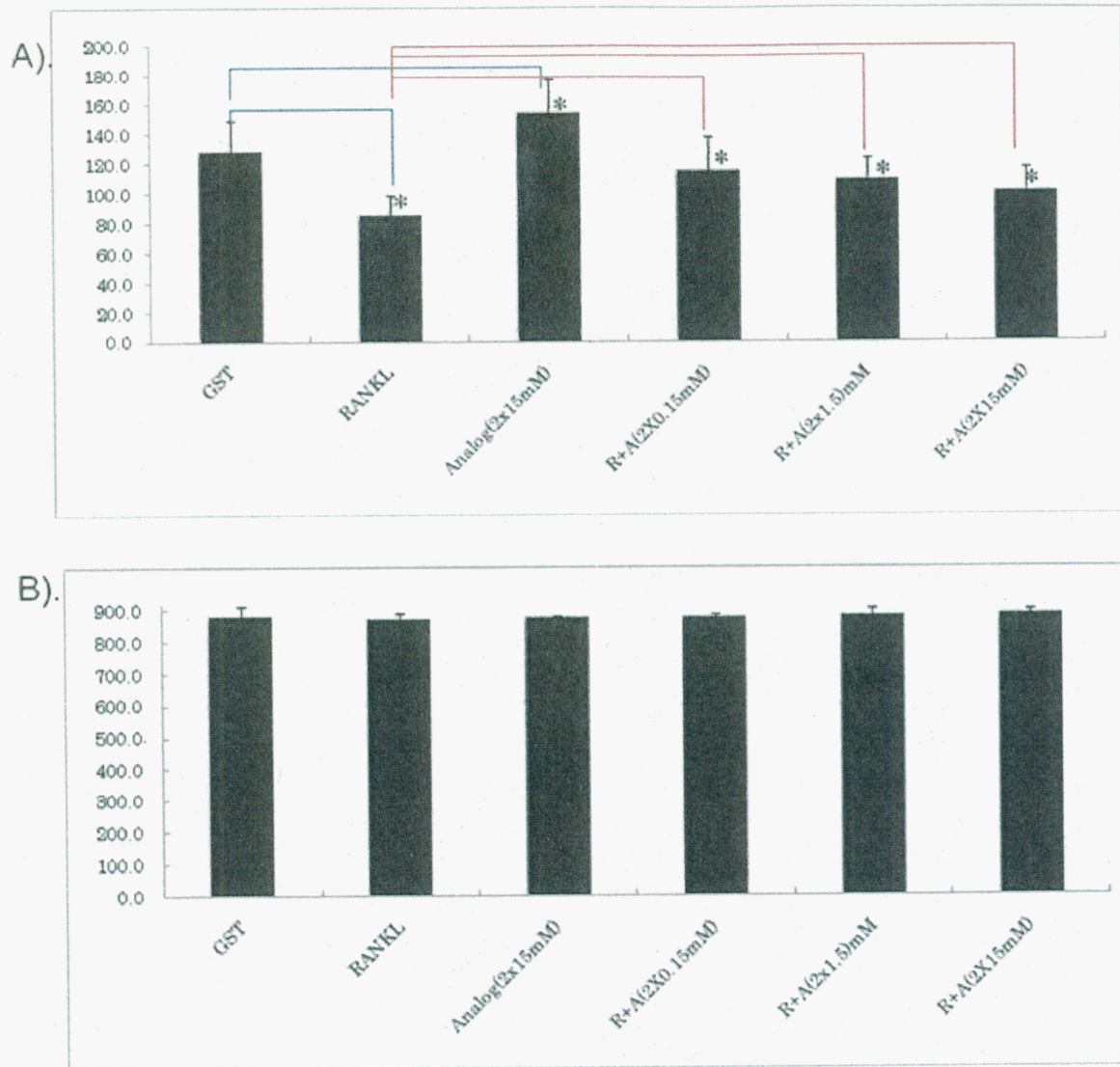


Figure 26. Effects of #290 on osteoporotic model mice.

Dosage effects of #290 on osteoporotic model mice. Indicated concentrations of #290 were injected intraperitoneally into mice treated as in figure 24 as well as untreated mice twice a day for three days, and bone density was measured. A) Trabecular bone B) Cortical bone

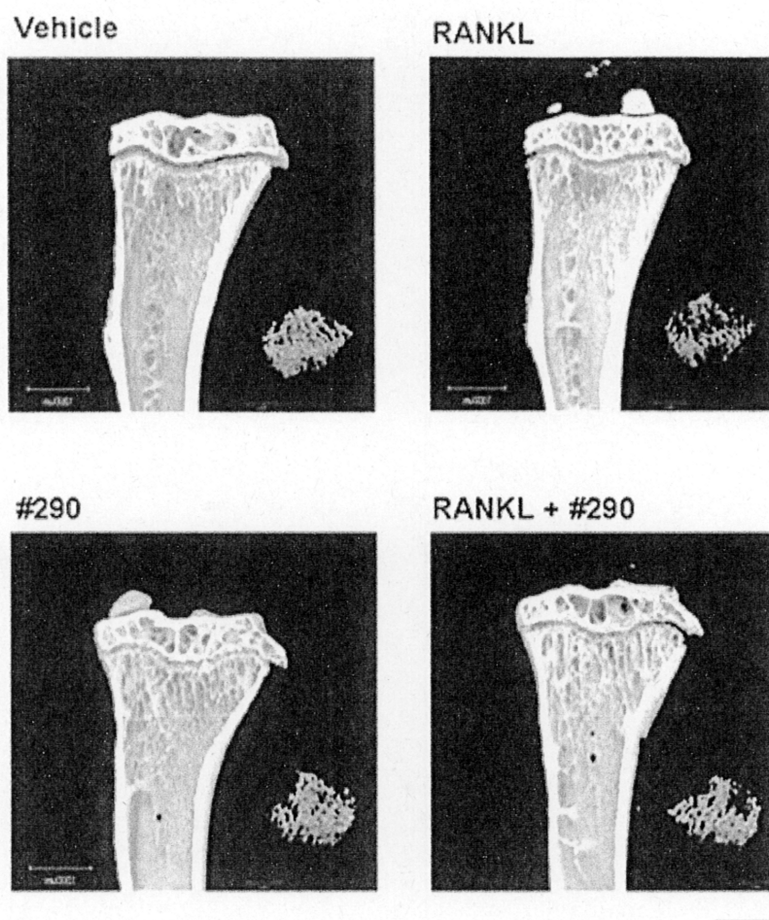


Figure 27. microCT analysis of Tibia.

Effects of RANKL-treatment and dosage of #290 on bone structure: micro-CT analysis. Tibiae of mice treated with RANKL (100 μ g) or/and #290 (15 mM) for four days was scanned by micro-CT and representative images are shown. Bar, 1,000 μ m.

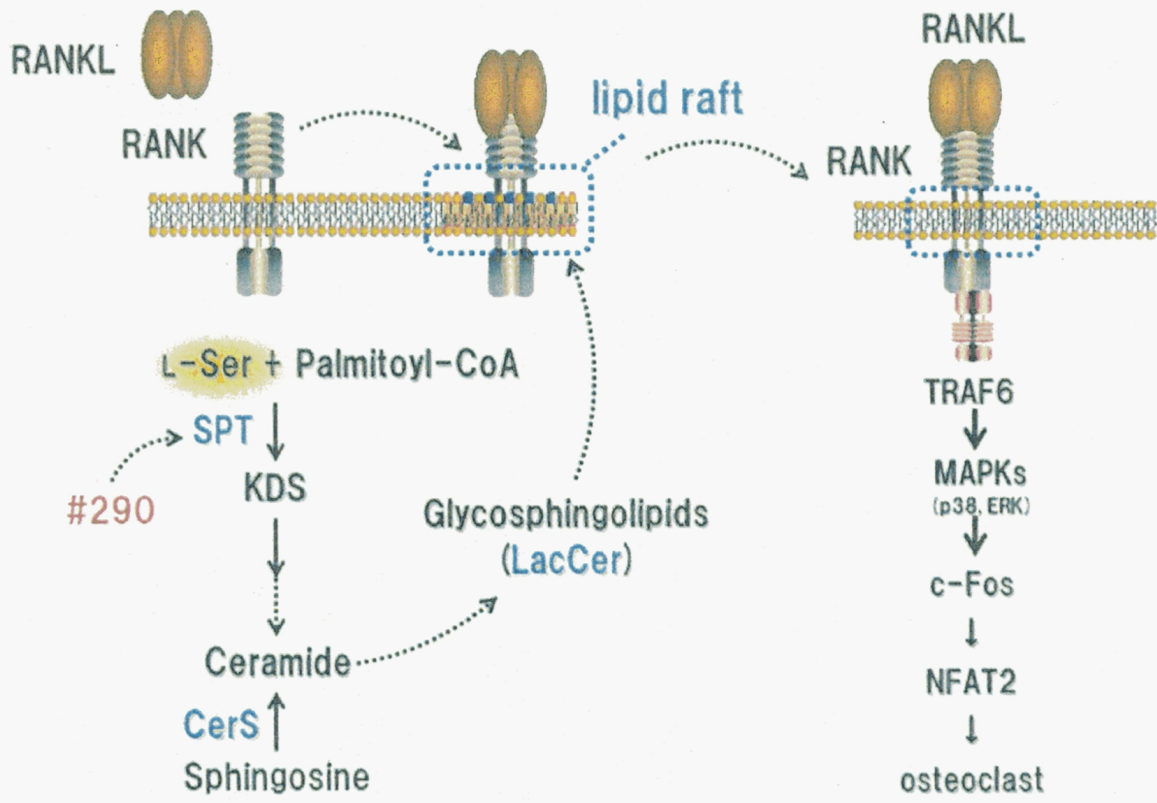


Figure 28. Proposed mechanism of action of #290

VI. Acknowledgements

In the name of Allah, the Most Gracious and the Most Merciful.

I wish to express my sincere thanks to Professor Tatsuo Takeya for his continuous guidance, invaluable discussions and encouragement throughout this study.

I would like to thank Dr. Norihiro Ishida-Kitagawa and Dr. Takuya Ogawa, for technical advice and any kind of help. And I also thank to all members of Laboratory of Molecular oncology, Nara Institute of Science and Technology, especially Dr. Shintaro Koga, Dr. Akiyama Motofusa, Nakamura Takahashi, Mai Nitta, for their continuous supports and friendships.

I would like to thanks Ministry of Education, Culture and Science of Japan for financial support and invaluable education opportunity.

I would like to give my sincere thanks to Mrs. Sachiko Iida for financial support and your thoughtfulness.

I would like to express my thankful to my family and my wife for their encourage me to reach a high level of education and never stop praying for me.

All praise to Allah, the Creator of the universe.

January, 2010

Anton Bahtiar

VII. References

- Akhila J, Deepa S, Alwar M (2007) Acute toxicity studies and determination of median lethal dose. *Current Science* 93:917-920.
- Aliprantis OA, Ueki Y, Sulyanto R, Park A, Sigrist KS, Sharma SM, Ostrowski MC, Olsen BR, Glimcher LH (2008) NFATc1 in mice represses osteoprotegerin during osteoclastogenesis and dissociates systemic osteopenia from inflammation in cherubism J. *Clin. Invest.* 118:3775–3789
- Asagiri M, Takayanagi H (2007) The molecular understanding of osteoclast differentiation. *Bone* 40:251-264
- Baeksgaard L., Andersen KP., Hyldstrup L (1998) Calcium and vitamin D supplementation increases spinal BMD in healthy, postmenopausal women. *Osteoporos Int* 8:255-260
- Boyle WJ, Simonet WS, Lacey DL (2003) Osteoclast differentiation and activation, *Nature* 423:337-342
- Boyce BF, Xing L (2008) Functions of RANKL/RANK/OPG in bone modeling and remodeling. *Arch Biochem Biophys* 473:139-146.
- Crotti, T.N., et al. (2008) PU.1 and NFATc1 mediate osteoclastic induction of the mouse beta3 integrin promoter. *J. Cell. Physiol.* **215**:636-644.
- Darnay BG, Haridas V, Ni J, Moore PA, Aggarwal BB (1998) Characterization of the intracellular domain of receptor activator of NF-KB (RANK). Interaction with tumor necrosis factor receptor-associated factors and activation of NF-KB and c-Jun N-terminal kinase, *J. Biol. Chem.* **273**:20551–20555
- Darnay BG, Ni J, Moore PA, Aggarwal BB (1999) Activation of NF-KB by RANK requires tumor necrosis factor receptor-associated factor (TRAF) 6 and NF-κB-inducing kinase. Identification of a novel TRAF6 interaction motif, *J. Biol. Chem.* **274**: 7724–7731
- Deng L, Wang C, Spencer E, Yang L, Braun A, You J (2000) Activation of the IKB kinase complex by TRAF6 requires a dimeric ubiquitin-conjugating enzyme complex and a unique polyubiquitin chain, *Cell* **103**:351–361.

Dunlop, DS, Neidle, A, McHale, D, Dunlop, DM, Lajtha, A (1986) "The presence of free D-aspartic acid in rodents and man" *Biochem Biophys Res Commun* 141: 27-32

Fukumoto S, Iwamoto T, Sakai E, Yuasa K, Fukumoto E, Yamada A, Hasegawa T, Nonaka K, Kato Y (2006) *Journal of Pharmacological Sciences*. 100:195-200

Eastell R (1996) Assessment of bone density and bone loss, *Osteoporos Int* 2 (suppl):S3-S5

Frost HM (1995) Osteoporosis: A rationale for further definitions. *Calcif Tissue Int* 62:89-94

Galibert L, Tometsko ME, Anderson DM, Cosman D, Dougall WC (1998) The involvement of multiple tumor necrosis factor receptor (TNFR)-associated factors in the signaling mechanisms of receptor activator of NF- κ B, a member of the TNFR superfamily, *J. Biol. Chem.* 273: 34120–34127.

Geddes AD, D'Souza SM, Ebetino FH, Ibbotson KJ (1994) Biphosphonates: structure-activity relationship and therapeutic implications, *J bone Miner res* 8:265-305

George GHM, MacGregor AJ, Spector TD (1999) Influence of current and past hormone replacement therapy on bone mineral density: study of discordant postmenopausal twins. *Osteoporos Int* 9:158-162

Gohda J, Akiyama T, Koga T, Takayanagi H, Tanaka S, Inoue J (2005) RANK-mediated amplification of TRAF6 signaling leads to NFATc1 induction during osteoclastogenesis, *EMBO J.* 24: 790–799

Gorai I, Chaki O, Taguchi Y, Nakayama m, Osada H, Suzuki N, Katagiri N, Misu Y, Minaguchi H (1999) Early postmenopausal bone loss is prevented by estrogen and partially by 1-OH-vitamin D3. *Calcif Tissue Int* 58:409-414

Hanada K, Hara T, Fukasawa M, Yamaji A, Umeda M, Nishijima M (1998) Mammalian cell mutants resistant to a sphingomyelin-directed cytolysin. Genetic and biochemical evidence for complex formation of the LCB1 protein with the LCB2 protein for serine palmitoyltransferase. *J Biol Chem* 273:33787-33794.

Hanada K, Hara T, Nishijima M (2000) D-serine inhibits serine palmitoyltransferase, the enzyme catalyzing the initial step of sphingolipids biosynthesis. *FEBS Lett* 474:63-65.

- Hanada K, Hara T, Mishijima M (2000) Purification of the serine palmitoyltransferase complex responsible for sphingolipids base synthesis by using affinity peptide chromatography techniques. *J Biol Chem* 275:8409-8415.
- Hannun YA, Obeid LM (2008) Principles of bioactive lipid signaling: lesson from sphingolipids. *Nature Review Molecular Cell Biology* 9:139-150
- Hashimoto, A, Nishikawa, T, Oka, T, Takahashi, K (1993) "Endogenous D-serine in rat brain: N-methyl-D-aspartate receptor-related distribution and aging" *J Neurochem* 60: 783-786
- Hill PA (1998) Bone remodeling. *British Journal of Orthodontics* 25:101-107
- Ichihara, A. and Greenberg, D.M. (1957) Further studies on the pathway of serine formation from carbohydrate. *J. Biol. Chem.* **224**, 331–340
- Hirabayashi Y, Furuya S (2008) Roles of L-serine and sphingolipids synthesis in brain development and neuronal survival. *Progress Lipid Res* 47:188-203.
- Ikeda F, Nishimura R, Matsubara T, Tanaka S, Inoue J, Reddy SV (2004) Critical roles of c-Jun signaling in regulation of NFAT family and RANKL-regulated osteoclast differentiation, *J. Clin. Invest.* **114**:475–484
- Inoue J, Ishida T, Tsukamoto N, Kobayashi N, Naito A, Azuma S (2000) Tumor necrosis factor receptor-associated factor (TRAF) family: adapter proteins that mediate cytokine signaling, *Exp. Cell Res.* **254**:14–24
- Ishida N, Hayashi K, Hoshijima M, Ogawa T, Koga S, Miyatake Y, Kumegawa M, Kimura Takeya T (2002) Large scale gene expression analysis of osteoclastogenesis in vitro and elucidation of NFAT2 as a key regulator. *J Biol Chem* 277:41147-41156
- Ishida N, Hayashi K, Hattori A, Yogo K, Kimura T, Takeya T (2006) CCR1 acts downstream of NFAT2 in osteoclastogenesis and enhances cell migration. *J Bone Miner Res* 21:48-57
- Iwamoto T, Fukumoto S, Kanaoka K, Sakai E, Shibata M, Fukumoto E, Inokuchi J, Takamiya K, Furukawa K, Furukawa K, Kato Y, Mizuno A (2001) Lactosylceramide is essential for the osteoclastogenesis mediated by macrophage-colony-stimulating factor and receptor activator of nuclear factor- κ B ligand. *J Biol Chem* 276:46031-46038.

- Kim K, Lee SH, Kim J, Choi, Y, Kim N (2008) NFATc1 induces osteoclast fusion via up-regulation of Atp6v0d2 and the dendritic cell-specific transmembrane protein (DC-STAMP). *Mol. Endocrinol.* **22**:176-185.
- Kitatani K, Idkowiak-Baldys J, Hannum YA (2008) The sphingolipids salvage pathway in ceramide metabolism and signaling. *Cell Signal* 20:1010-1018.
- Kobayashi N, Kadono Y, Naito A, Matsumoto K, Yamamoto T, Tanaka S (2001) Segregation of TRAF6-mediated signaling pathways clarifies its role in osteoclastogenesis, *EMBO J.* **20**:1271–1280.
- Lloyd SAJ, Yuan YY, Kostenuik PJ, Ominsky MS, Lau AG, Morony S, Stolina M, Asuncion FJ, Bateman TA (2008) Soluble RANKL induces high bone turnover and decreases bone volume, density, and strength in mice. *Calcif Tissue Int* 82:361-372.
- Lomaga MA, Yeh WC, Sarosi I, Duncan GC, Furlonger C, Ho A (1999) TRAF6 deficiency results in osteopetrosis and defective interleukin-1, CD40, and LPS signaling, *Genes Dev.* **13**: 1015–1024
- Merrill Jr. AH (1983) Characterization of serine palmitoyltransferase activity in Chinese hamster ovary cells. *Biochim Biphys Acta* 754:284-291. Mizukami J, Takaesu G, Akatsuka H, Sakurai H, Ninomiya-Tsuji J, Matsumoto K (2002) Receptor activator of NF- κ B ligand (RANKL) activates TAK1 mitogen-activated protein kinase kinase through a signaling complex containing RANK, TAB2, and TRAF6, *Mol. Cell. Biol.* **22**: 992–1000.
- Ogawa T, Ishida-Kitagawa N, Tanaka A, Matsumoto T, Hirouchi T, Akimaru M, Tanihara M, Yogo K, Takeya T (2006) A novel role of L-serine (L-Ser) for the expression of nuclear factor of activated T cells (NFAT)2 in receptor activator of nuclear factor κ B ligand (RANKL)-induced osteoclastogenesis in vitro. *J Bone Miner Metab* 24:373-379.
- Ogretmen B, Hannum YA (2004) Biologically active sphingolipids in cancer ; pathogenesis and treatment. *Nature Review Cancer* 4: 604-614
- Schell, MJ (2004) "The N-methyl-D-aspartate receptor glycine site and D-serine metabolism: an evolutionary perspective" *Phil Trans R Soc London* 359: 943-964
- Scolari MJ, Acosta GB (2007) D-serine: a new world in the glutamatergic neuroglial language. *Amino acids* 33:563-574

Snell, K. (1984) Enzymes of serine metabolism in normal, developing and neoplastic rat tissues. *Adv. Enzyme Regul.* **22**, 325–400

Sommerfeldt DW, Rubin CT (2001) Biology of bone and how it orchestrates the form and function of the skeleton. *Eur Spine J* 10:86-95

Soto A, DelRaso NJ, Schlager JJ, Chan VT (2008) D-serine exposure resulted in gene expression changes indicative of activation of fibrogenic pathways and down-regulation of energy metabolism and oxidative stress response. *Toxicology* 243:177-192.

Takayanagi H (2007) Osteoimmunology: shared mechanisms and crosstalk between the immune and bone systems. *Nature Reviews Immunology* 7 : 292-304

Takayanagi H, Kim S, Koga T, Nishina S, Isshiki M, Yoshida H (2002) Induction and activation of the transcription factor NFATc1 (NFAT2) integrate RANKL signaling for terminal differentiation of osteoclasts, *Dev. Cell* **3**:889–901.

Tanaka S, Nakamura K, Takahashi N, Suda T (2005) Role of RANKL in physiological and pathological bone resorption and therapeutic targeting the RANKL-RANK signaling system. *Immunol Rev* 208:30-49.

Teitelbaum SL (2007) Osteoclasts: what do they do and how do they do it? *Am J Pathol* 170:427-435.

Theill LE, Boyle WJ, Penninger JM (2002) RANK-L and RANK: T cells, bone loss, and mammalian evolution, *Annu. Rev. Immunol.* **20**, 795–823.

Väänänen HK, Laitala-Leinonen T (2008) Osteoclast lineage and function. *Arch Biochem Biophys* 473:132-138.

Wagner EF, Eferl R (2005) Fos/AP-1 proteins in bone and the immune system, *Immunol. Rev.* **208**:126–140

Williams RD, Wang E, Merrill AH (1984) Enzymology of long-chain base synthesis by liver: characterization of serine palmitoyltransferase in rat liver microsomes. *Arch Biochem Biophys* 228:282-291.

Wolosker H, Dumin E, Balan L, Foltyn VN (2008) D-amino acids in the brain: D-serine in neurotransmission and neurodegeneration. *FEBS J* 275:3514-3526.

Wovern N, Gotfredsen K (2001) Implant-supported over-dentures, a prevention of bone loss in edentulous mandibles? *Clin Oral Impl res* 12:113-124

Wong BR, Josien R, Lee SY, Vologodskaja M, Steinman R, Choi M (1998) The TRAF family of signal transducers mediates NF- κ B activation by the TRANCE receptor, *J Biol Chem* 273:28355–28359

Yoshida H, Hayashi S, Kunisada T, Ogawa M, Nishikawa S, Okamura H (1990) The murine mutation osteopetrosis is in the coding region of the macrophage colony stimulating factor gene, *Nature* 345: 442–444

Yoshida K, Furuya S, Osuka S, Mitoma J, Shinoda Y, Watanabe M, Azuma N, Tanaka H, Hashikawa T, Itohara S, Hirabayashi Y (2004) Targeted disruption of the mouse 3-phosphoglycerate dehydrogenase gene causes severe neurodevelopmental defects and results in embryonic lethality. *J Biol Chem* 279:3573-3577